ORIGINAL CONTRIBUTION

CrossMark

Vagus nerve stimulation exerts cardioprotection against myocardial ischemia/reperfusion injury predominantly through its efferent vagal fibers

Watthana Nuntaphum[1,2,3] · Wanpitak Pongkan[1,2,3] · Suwakon Wongjaikam[1,2,3] · Savitree Thummasorn[1,2,3] · Pongpan Tanajak[1,2,3] · Juthamas Khamseekaew[1,2,3] · Kannaporn Intachai[1,2,3] · Siriporn C. Chattipakorn[1,2,3,4] · Nipon Chattipakorn[1,2,3] · Krekwit Shinlapawittayatorn[1,2,3] (ORCID)

Abstract

Vagus nerve stimulation (VNS) has been shown to exert cardioprotection against myocardial ischemia/reperfusion (I/R) injury. However, whether the cardioprotection of VNS is mainly due to direct activation through its ipsilateral efferent fibers (motor) rather than indirect effects mediated by the afferent fibers (sensory) have not been clearly understood. We hypothesized that VNS exerts cardioprotection predominantly through its efferent vagal fibers. Thirty swine (30–35 kg) were randomized into five groups: I/R no VNS (I/R), and left mid-cervical VNS with both vagal trunks intact (LC-VNS), with left vagus nerve transection (LtVNX), with right vagus nerve transection (RtVNX) and with atropine pretreatment (Atropine), respectively. VNS was applied at the onset of ischemia (60 min) and continued until the end of reperfusion (120 min). Cardiac function, infarct size, arrhythmia score, myocardial connexin43 expression, apoptotic markers, oxidative stress markers, inflammatory markers (TNF-α and IL-10) and cardiac mitochondrial function, dynamics and fatty acid oxidation (MFN2, OPA1, DRP1, PGC1α and CPT1) were determined. LC-VNS exerted cardioprotection against myocardial I/R injury via improvement of mitochondrial function and dynamics and shifted cardiac fatty acid metabolism toward beta oxidation. However, LC-VNS and LtVNX, both efferent vagal fibers are intact, produced more profound cardioprotection, particularly infarct size reduction, decreased arrhythmia score, oxidative stress and apoptosis and attenuated mitochondrial dysfunction compared to RtVNX. These beneficial effects of VNS were abolished by atropine. Our findings suggest that selective efferent VNS may potentially be effective in attenuating myocardial I/R injury. Moreover, VNS required the contralateral efferent vagal activities to fully provide its cardioprotection.

Keywords Vagus nerve stimulation · Efferent fiber · Ischemic/reperfusion injury · Cardioprotection

✉ Krekwit Shinlapawittayatorn
kshinlap@gmail.com

1 Faculty of Medicine, Cardiac Electrophysiology Research and Training Center, Chiang Mai University, Chiang Mai 50200, Thailand

2 Cardiac Electrophysiology Unit, Department of Physiology, Faculty of Medicine, Chiang Mai University, Chiang Mai 50200, Thailand

3 Center of Excellence in Cardiac Electrophysiology Research, Chiang Mai University, Chiang Mai 50200, Thailand

4 Department of Oral Biology and Diagnostic Sciences, Faculty of Dentistry, Chiang Mai University, Chiang Mai 50200, Thailand

Introduction

Acute myocardial infarction (AMI) is a major cause of morbidity and mortality worldwide [59]. Although early and rapid reperfusion is the most effective strategy to reduce myocardial injury and limit the infarct size, reperfusion itself can induce cardiomyocyte death. This phenomenon is known as myocardial ischemia/reperfusion (I/R) injury [59]. During I/R, reactive oxygen species (ROS) is dramatically increased [31], which causes oxidative damage and cell apoptosis [43]. Moreover, I/R injury can induce mitochondrial dysfunction and structural change including impaired mitochondrial dynamics and metabolism [11]. These deleterious effects lead to myocardial cell death, increased infarct size, cardiac arrhythmia and impaired left ventricular and

🖄 Springer

hemodynamic parameters [46, 47]. Therefore, cardioprotection beyond that by timely reperfusion is needed to reduce infarct size and improve the prognosis of the affected AMI patients [26]. Previous study demonstrated that myocardial infarction increases sympathetic tone, especially the relative ischemia distal to a severe coronary stenosis which in turn results in poststenotic vasoconstriction and an aggravation of ischemia, and decreases parasympathetic tone [28]. Therefore, rebalanced autonomic activity by augmenting vagal activity may be a potential therapeutic intervention for the affected MI patients. A growing body of literature has shown that enhancing parasympathetic activity by electrical stimulation of the cervical vagus nerve (both afferent and efferent fibers) has emerged as a promising therapy for various conditions, including brain and heart diseases [15, 44]. Specifically in the heart, both invasive and non-invasive vagus nerve stimulations (VNS) have been shown to exert cardioprotection in patients with chronic heart failure (the ANTHEM-HF trial) and ischemic heart diseases [22, 25, 27, 45, 60].

The vagus nerve is a mixed nerve which contains 80% afferent fibers (sensory) and 20% efferent fibers (motor) [61]. Recently, in I/R swine model, we have demonstrated that left cervical VNS (anode cephalad to cathode to stimulate cardiac efferent vagal fibers) applied at the onset or during the ischemic periods can improve cardiac function, decrease myocardial infarct size, reduce dispersion of repolarization via amelioration of cardiac mitochondrial dysfunction [46, 47]. Moreover, VNS (caudal end to stimulate cardiac efferent vagal fibers) can improve mitochondrial function through the activation of M_3 receptor/CaMKKβ/AMPK pathway in isoproterenol-induced cardiac damage in rats [55]. In addition, previous study demonstrated that VNS also activated the ipsilateral afferent vagal fibers, which reflexively reduced cardiac efferent parasympathetic effects [56]. Although VNS has been shown to exert cardioprotection against myocardial I/R injury in both preclinical and clinical studies, it is still remained unclear whether the cardioprotection of VNS is mainly due to direct vagal activation through its ipsilateral efferent vagal fibers (motor) or indirect effects mediated by the afferent vagal fibers (sensory). Additionally, the majority of publications describing cardioprotection by VNS were performed in small animals (rodents or rabbits), which are sympathetically dominant [18, 19]. However, the importance of vagal tone for the heart in small animal is less than that in larger mammals (canine or pigs) or humans [16]. Thus, it is important to study the role of vagus nerve activation in cardioprotection in a larger mammal model. Therefore, the objectives of this study were to determine whether the cardioprotective effects against myocardial I/R injury of VNS were mainly due to direct ipsilateral efferent vagal fibers activation or indirect effects mediated by the afferent vagal fibers in a large animal model of AMI. Furthermore, roles of

the contralateral efferent vagal fibers during VNS were also investigated. We hypothesized that VNS exerts cardioprotection against myocardial I/R injury predominantly through its ipsilateral efferent vagal fibers.

Methods

Animal preparation

All experiments were approved by the Institutional Animal Care and Use Committees of the Faculty of Medicine, Chiang Mai University, Chiang Mai, Thailand. Thirty domestic pigs (30–35 kg) were anesthetized by an intramuscular injection of a combination of 4.4 mg/kg zoletil® (Virbac Laboratories, Carros, France) and 2.2 mg/kg xylazine (Laboratorios Calier, S.A., Barcelona, Spain). After endotracheal intubation, anesthesia was maintained by 1.5–3.0% isoflurane (Abbott Laboratories Ltd., Queenborough, UK) delivered in 100% oxygen. Surface electrocardiogram (lead II), femoral arterial blood pressure (BP), heart rate (HR), and rectal temperature were continuously monitored, and all data were recorded for subsequent analysis. Arterial blood gases and electrolytes were also monitored every 30 min and maintained within acceptable physiological ranges [14]. Furthermore, under fluoroscopic guidance, platinum-coated titanium coil electrodes (34- and 68-mm) were advanced into and positioned at the right ventricular apex and the junction between the right atrium and superior vena cava, respectively, to deliver electrical shocks when malignant ventricular arrhythmias spontaneously occurred during I/R periods [14].

Ischemia/reperfusion (I/R) protocol

The heart was exposed through a left thoracotomy. The left anterior descending artery (LAD) were isolated and occluded by ligature (3–0 silk) 3 cm from the left main coronary artery. Ischemia was confirmed by an ST elevation on the ECG (lead II) and the change in color of myocardial tissues on the ischemic area. I/R were performed by 60 min of a complete LAD occlusion followed by 120 min of reperfusion.

### Vagus nerve stimulation (VNS) protocol

The left vagus nerve was surgically isolated (~ 3 cm length, at C5–C6 level) from the carotid sheath. A VNS lead (Model 304, Cyberonics, Houston, TX, USA) with bipolar electrodes (platinum–iridium, 4 mm² surface area, 6-mm interelectrode spacing) were attached to the vagus nerve using helical fixation elements to assure electrode stability. The cathodic electrode was oriented

closest to the heart. The proximal terminal pin of VNS lead was attached to a pulse generator (Demipulse, Model 103, Cyberonics) for delivery of VNS. Prior to onset of ischemia, the mean PR interval was determined from an average of ten consecutive sinus beats. We verified that VNS was engaging the autonomic nervous system by briefly stimulating the vagus nerve and observing a significant increase in the PR intervals. In the present study, we sought to determine whether the cardioprotection of VNS is mainly due to direct activation through its ipsilateral efferent fibers (motor) or through the indirect effects mediated by the afferent fibers (sensory) using infarct size as the primary endpoint. Thus, we intended to use the I/R protocol and the VNS parameters (3.5 mA, 500 μs pulse width, 20 Hz and continuous recurring cycles of 21-s ON and 30-s OFF) which provided the most potent anti-infarct effect (about 89% reduction) based on our previous studies [46, 47].

Experimental protocols

Pigs were randomly divided into five groups ($n=6$/group) as shown in Fig. 1. All pigs in each group were subjected to I/R protocol. Group 1 (I/R): pigs were sham operated without VNS. Group 2 (LC-VNS): the vagal nerve was left intact for combined afferent and efferent stimulations, pigs were received intermittent left cervical VNS at the onset of LAD occlusion and continued until the end of reperfusion. Group 3 (LtVNX): pigs were assigned to left vagus nerve transection at middle cervical level and received intermittent left cervical VNS 2 cm under the point of cut for selective efferent vagal nerve stimulation. Group 4 (RtVNX): to study the roles of the contralateral efferent vagal fibers during VNS, pigs were assigned to right vagus nerve transection at middle cervical level and received intermittent left cervical VNS. Group 5 (Atropine): pigs were received Atropine (1 mg/kg) by administered intravenous 15 min prior to initiation of left cervical VNS to inhibit parasympathetic actions on the heart.

Fig. 1 Schematic representation of the study protocols. **a** Diagram of the I/R induction surgery. The ischemic period (60 min) was induced by complete LAD coronary artery ligation, followed by 120 min of reperfusion. VNS was applied at the onset of the ischemic period. **b** Diagram of the experimental protocol. *I/R* ischemia/reperfusion, *LAD* left anterior descending, *LC-VNS* left cervical vagus nerve stimulation, *LtVNX* left vagus nerve transection, *RtVNX* right vagus nerve transection
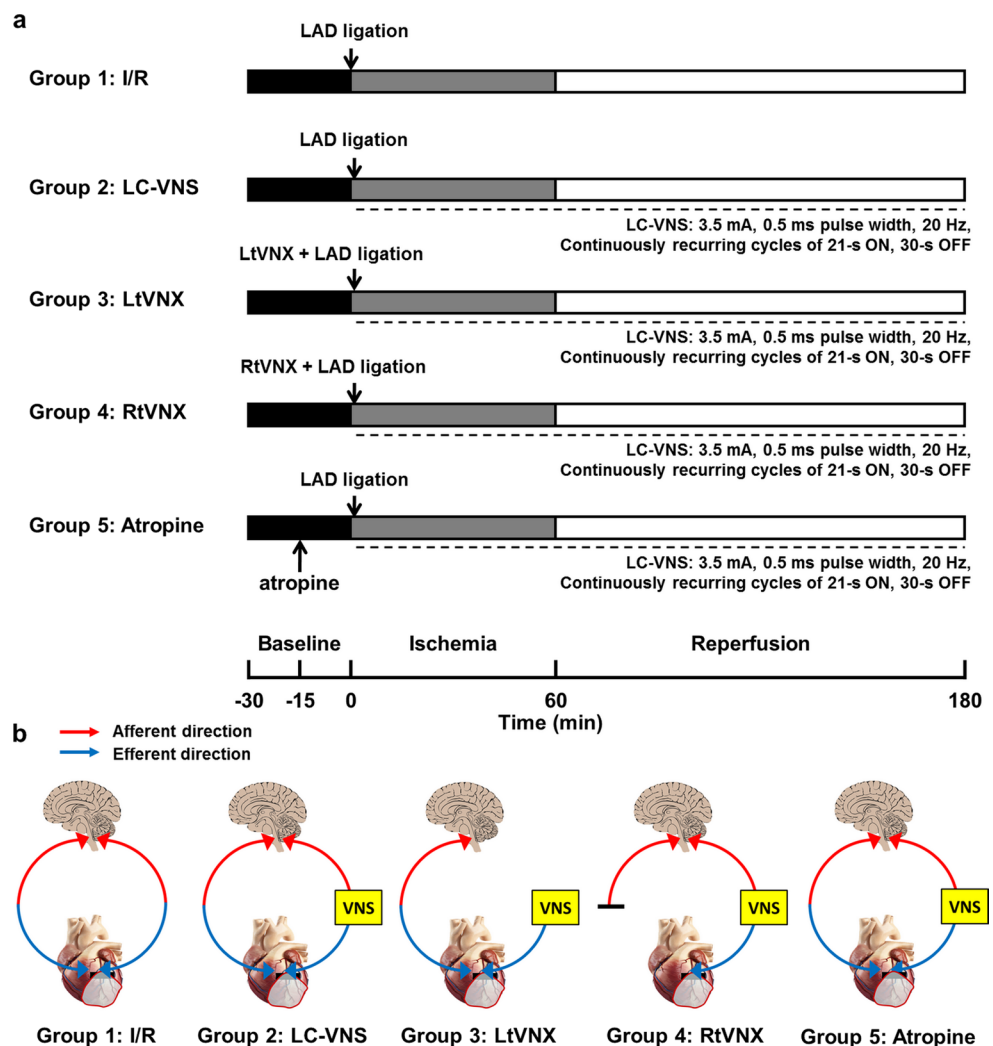
Evaluation of ECG parameters

Heart rate (HR), PR interval, QRS complex duration (an indicator of ventricular activation time), QT interval (an indicator of ventricular repolarization time), time from T-wave peak to end (Tpe; an indicator of transmural dispersion of repolarization), and T-wave peak to end per QT interval ratio (Tpe/QT ratio; an indicator of dispersion of repolarization relative to the total duration of repolarization) were measured. ECG traces were analyzed with Chart 6 (AD Instruments). The mean baseline all of parameters was determined from an average of twenty sinus beats just prior to LAD occlusion. The mean parameters during the ischemia and reperfusion periods were analyzed from an average of twenty consecutive beats before the end of occlusion and the end of reperfusion, respectively.

Evaluation of rhythm disturbances

Premature ventricular contractions (PVC), ventricular tachycardia (VT), and ventricular fibrillation (VF) were defined according to the Lambeth Convention criteria [17] with more rigorous modifications for the entire 180 min I/R period. Specifically, PVC was defined as ventricular contractions without atrial depolarization. VT was defined as more than six consecutive PVC. VF was characterized by a loss of synchronicity of electrocardiogram plus decreased amplitude and a precipitous fall in blood pressure (BP) for more than one second. ECG traces were analyzed with Chart 6 (AD Instruments). Furthermore, the arrhythmia scores and mortality rate were determined. The arrhythmia scores all correlated with the incidences of PVC, VT, and VF [8].

Evaluation of left ventricular (LV) function parameters

During the I/R periods, the left ventricular function including stroke volume (SV), ejection fraction (EF), end-systolic pressure (ESP), and end-diastolic pressure (EDP), and stroke work (SW) were continuously monitored and recorded using the pressure–volume (P–V) loop recording system (Model ADV500/ADVantage System, Scisense Inc., London, Canada) as described previously [40].

Infarct size determination

After 120 min of reperfusion, the LAD were re-occluded by the LAD ligation, and the heart was removed and irrigated with normal saline to wash out blood from chambers and vessels. The infarct size was assessed with 0.5% Evans Blue and 1.0% triphenyltetrazolium chloride (TTC) staining as previously described [47]. The area at risk (AAR) was defined as the area not stained by the Evan blue dye, and the infarcted area was defined as the area not stained by TTC. An area measurement was performed using the Image Tool software version 3.0. The area of infarct size was normalized to the AAR and calculated as %infarct size/AAR as described previously [47].

Isolated cardiac mitochondria

Cardiac mitochondria were isolated from the ischemic and non-ischemic regions, using the technique previously described [50], and the protein concentration was determined according to the bicinchoninic acid assay. Cardiac mitochondrial functions were determined by measuring the cardiac mitochondrial reactive oxygen species (ROS) production, cardiac mitochondrial membrane potential change ($\Delta\Psi$m) and cardiac mitochondrial swelling. Cardiac mitochondrial ROS production was determined using a fluorescent microplate reader in all groups. The dye dichloro-dihydro-fluorescein diacetate (DCFDA) was used to determine the level of ROS production in cardiac mitochondria. The DCFDA can pass through the mitochondrial membrane, and was oxidized by ROS in the mitochondria into the fluorescent form of DCF. Thus, increased fluorescent intensity indicates increased ROS production in the mitochondria. A cardiac mitochondrial membrane potential change was determined using a fluorescent microplate reader in all groups. The dye 5,5′,6,6′-tetrachloro-1,1′,3,3′-tetraethyl-benzimidazolcarbocyanine iodide (JC-1) was used to determine the change in the mitochondrial membrane potential. JC-1 is characterized as a cation and remains in the mitochondrial matrix as a monomer (green fluorescence) form. However, it can interact with anions in the mitochondrial matrix to form an aggregate (red fluorescence) form. Cardiac mitochondrial depolarization was indicated by a decrease in the red/green fluorescence intensity ratio. Cardiac mitochondrial swelling was assessed by measuring changes in the absorbance of the suspension wavelength at 540 nm using a microplate reader. Cardiac mitochondria (0.4 mg/ml) were incubated in 2 ml of respiration buffer: KCl 150 mM, HEPES 5 mM, $K_2HPO_4 \cdot 3H_2O$ 5 mM, L-glutamate 2 mM and pyruvate sodium salt 5 mM. Mitochondrial swelling was indicated by a decrease in the absorbance of the mitochondrial suspension. Isolated cardiac mitochondrial morphology was confirmed using a transmission electron microscope.

Transmission electron microscopy for cardiac mitochondrial morphology

Cardiac mitochondrial morphology was determined by transmission electron microscopy. Isolated cardiac mitochondria from both ischemic and remote areas were fixed overnight by mixing 2.5% glutaraldehyde in 0.1 M cacodylate buffer, pH 7.4 at 4 °C. Then, the pellets were post

fixed in 1% cacodylate-buffered osmium tetroxide for 2 h at room temperature. The pellets were dehydrated in a graded series of ethanol and embedded in Epon-Araldite and cut by a diamond knife into ultra-thin sections (60–80 nm thick), placed on copper grids and stained with the combination of uranyl acetate and lead citrate. Finally, the mitochondrial morphology was observed with a transmission electron microscope [58].

Western blot analysis

At the end of each experiment, the hearts were rapidly excised, and then the remote and ischemic areas of ventricular tissues were collected, quickly frozen in liquid nitrogen, and stored at -80 °C until analysis. Heart proteins were lysed with extraction buffer (Tris–HCl 20 mmol/l, Na_3VO_4 1 mmol/l, and NaF 5 mmol/l) and separated by electrophoresis on 10% sodium dodecyl sulfate-polyacrylamide gel electrophoresis, and then were transferred onto nitrocellulose membranes. After immunoblots were blocked for 1 h with 5% nonfat dry milk in Tris-buffer saline (pH 7.4) containing 0.1% Tween 20, they were probed overnight at 4 °C with the primary antibodies that recognize phospho-connexin43 (P-Cx43)(Ser 368) and total connexin43 (Total-Cx43) (1:1000 dilution, Cell Signaling Technology, Danvers, MA, USA); a marker of intercellular electrical communication, Bax, Bcl-2, Pro caspase-3 and Cleaved caspase-3 (1:1000 dilution, Cell Signaling Technology, Danvers, MA, USA); a marker of apoptosis, Mitofusin-2 (MFN2), optic atrophy protein 1 (OPA1), dynamin-related protein 1 (DRP1), phospho-dynamin-related protein 1 at serine 616 (P-DRP1 Ser 616) and serine 637 (P-DRP1 Ser 637) (1:1000 dilution, Cell Signaling Technology, Danvers, MA, USA); a marker of mitochondrial fission and fusion, phospho-AMPK-activated protein kinase (P-AMPK) and total AMPK (1:1000 dilution, Cell Signaling Technology, Danvers, MA, USA); a marker of cardiac cellular energy homeostasis, peroxisome proliferator-activated receptor-gamma coactivator 1 alpha (PGC1α), carnitine palmitoyltransferase 1 (CPT1) (1:200 dilution, Santa Cruz biotechnology, TX, USA); a marker of mitochondrial biogenesis and fatty acid oxidation, mitochondrial complex I–V (1:2000 dilution, Cell Signaling Technology, Danvers, MA, USA); a marker of cardiac mitochondrial respiration and actin (1:4000 dilution, Santa Cruz biotechnology, TX, USA); a loading control, followed by 1 h of incubation at room temperature with the horseradish peroxidase-conjugated secondary antibody (1:2000 dilution, Cell Signaling Technology, Danvers, MA, USA). The blots were visualized by ECL reagent (Bio-Rad Laboratories, CA, USA). The western blot pictures were carried out using the ChemiDoc Touching system (Bio-Rad Laboratories, CA, USA). The densitometric analysis was performed using NIH Image J analysis software. For quantitation of the proteins of interest, the ratio of ischemic (I) area per remote (R) area was determined, and normalized with actin.

HPLC-based assay of malondialdehyde (MDA) concentration

Malondialdehyde (MDA) concentration in cardiac tissue was measured by HPLC system [37]. A 0.5 ml aliquot of samples were mixed with 1.1 ml of 10% trichloroacetic acid (TCA) containing BHT (50 ppm), heated at 90 °C for 30 min and cooled down to room temperature. The mixture was centrifuged at 6000 rpm, 10 min. The supernatant (0.5 ml) was mixed with 0.44 M H_3PO_4 (1.5 ml) and 0.6% thiobarbituric acid (TBA) solution (1.0 ml) and then incubated at 90 °C for 30 min to generate a pink-colored products called thiobarbituric acid reactive substances (TBARS). The solution was filtered through a syringe filter (polysulfone-type membrane, pore size 0.45 μm, Whatman International, Maidstone, United Kingdom) and analyzed with HPLC system. The TBARS was fractionated on the adsorption column (Water Spherisorb ODS2 type, 250×4.3 mm, 5 μm), eluted with mobile-phase solvent of 50 mM KH_2PO_4: methanol at flow rate 1.0 ml/min and online detected at 532 nm. Data were recorded and analyzed with BDS software (BarSpec Ltd., Rehovot, Israel). A standard curve was constructed from the peak from height of standard 1,1,3,3-tetramethoxypropane (standard reagent for malondialdehyde) at different concentrations (0–10 μM). TBARS concentration was determined directly from standard curve and reported as MDA equivalent concentration. MDA concentration was expressed in μM [37].

Cardiac inflammatory and anti-inflammatory cytokine assay

Myocardial protein was extracted by the homogenization of myocardial tissues in a homogenization buffer (PBS containing 0.5% Triton X-100 and a protease inhibitor cocktail, pH 7.2 at 4 °C), and subsequently be centrifuged at 14,359g for 10 min. Then, the supernatant and plasma were collected to measure the level of tumor necrosis factor-α (TNF-α) and interleukin-10 (IL-10), a marker of pro-inflammatory and anti-inflammatory cytokines, using an enzyme-linked immunosorbent assay (ELISA) kit (Biosource International, Inc., Camarillo, CA, USA).

TUNEL

To quantitatively determine cardiomyocyte apoptosis, TUNEL staining (terminal Deoxynucleotidyl transferase-mediated dUTP nick end labeling) was performed. TUNEL staining of cardiomyocyte was performed with a TdT Blue Label apoptosis detection kit. The enzyme

terminal deoxynucleotidyl transferase was used to incorporate biotinylated-conjugated dUTP to the ends of DNA fragments. At the end of the experiment, the hearts were perfused first with 0.9% NaCl for 5 min and then with 4% paraformaldehyde in PBS (pH 7.4) for 20 min. The ventricles were removed and further fixed in 4% paraformaldehyde in PBS (pH 7.4) for 20 h at room temperature. The ventricles were cut into 10 μm sections for the TUNEL assay in a cryostat. Immunohistochemical procedures for detecting apoptotic cardiomyocytes were performed using an In Situ Apoptosis Detection Kit (Trevigen, Maryland, USA) according to the manufacturer's instructions. For the negative control, TdT was omitted from the reaction mixture. After washing, the label incorporated at the damaged sites of the DNA was visualized by fluorescence microscopy. Five images per heart (3–5 hearts per genotype group) were acquired and positive cells were counted individually. Results were expressed as the percentage of apoptotic cells among the total cell population [33].

Statistical analysis

Data were expressed as mean ± standard error. The normality and equality of variance were tested using the Shapiro–Wilk test and Levene's test, respectively. For mortality rate, differences between groups were evaluated with Chi-square test followed by Bonferroni correction. The mean values between the two groups were compared using the paired student's t-test. One-way ANOVA with Dunnett's multiple-comparison or LSD tests using the statistical program SPSS22 (SPSS, Inc., Chicago, IL, USA) were used for multiple sets of data. A value of $p < 0.05$ was considered statistically significant.

Results

Effects of VNS on the ECG parameters during I/R

Figure 2a shows examples of ECG tracing at baseline, a marked elevation of the ST segment after 5 min of LAD
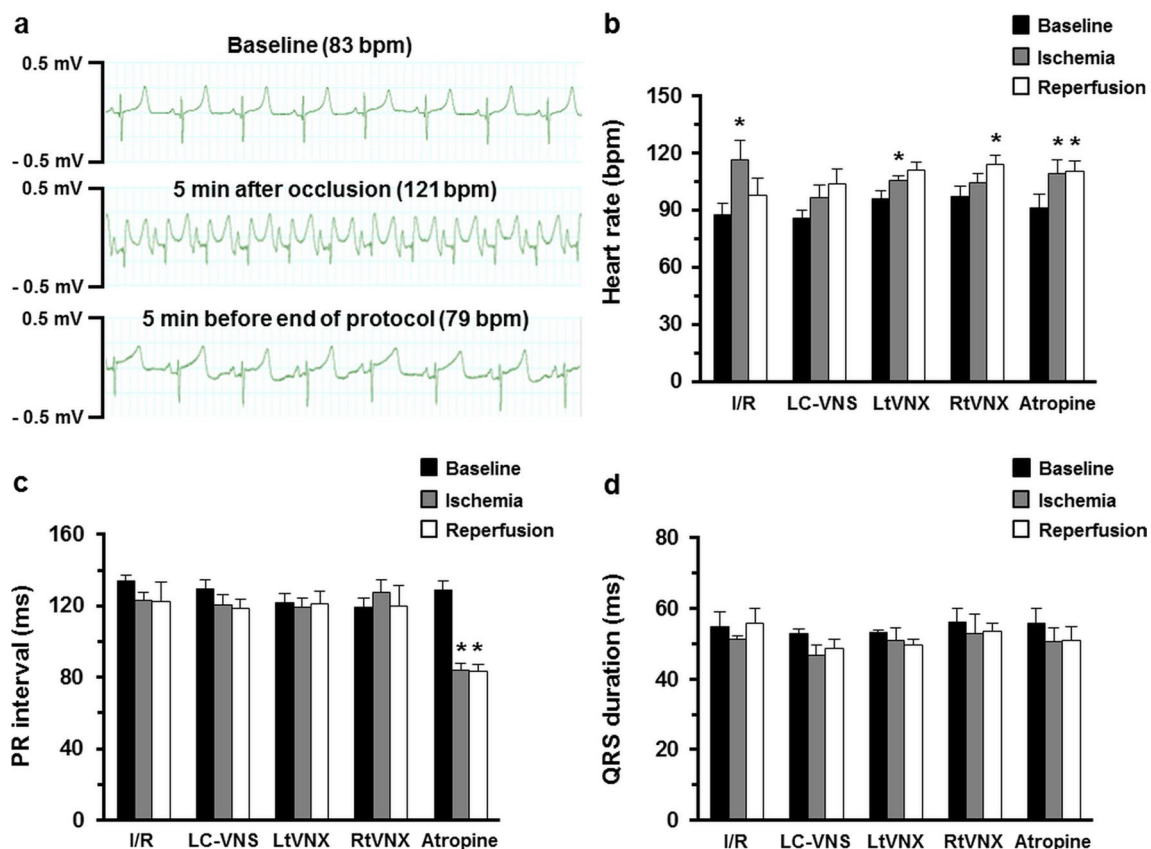
Fig. 2 The electrocardiographic parameters during the ischemic and the reperfusion periods. **a** Representative ECG at the baseline, 5 min after LAD ligation and 5 min before end of reperfusion. **b** Effects of VNS on the heart 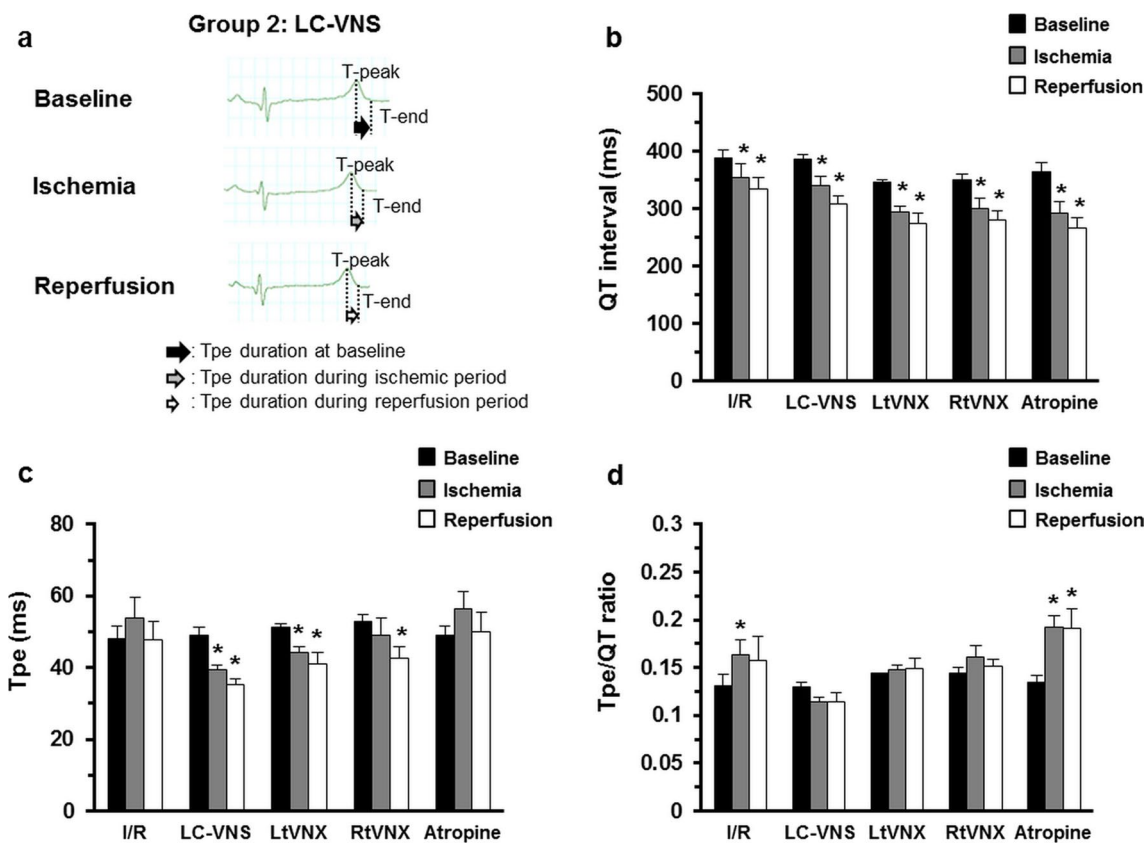rate. **c** Effects of VNS on the mean PR interval. **d** Effects of VNS on the mean QRS duration. Data are presented as mean ± SE. *$p < 0.05$ vs baseline within group. *I/R* ischemia/reperfusion, *LC-VNS* left cervical vagus nerve stimulation, *LtVNX* left vagus nerve transection, *RtVNX* right vagus nerve transection

occlusion and ECG tracing returned to baseline after reperfusion. The electrophysiological effects of VNS were examined in 30 pigs in which heart rate (HR), PR interval, QRS duration, QT interval, T-wave peak to end (Tpe), and Tpe/QT ratio were continuously measured during the I/R period. In I/R group, HR during the ischemic period increased significantly compared with the baseline and returned to the baseline after reperfusion (Fig. 2b). HR at the baseline, during ischemia, and reperfusion periods was not different in all VNS-treated groups. Interestingly, HR significantly increased in the LtVNX group during ischemia. In contrast, HR significantly increased during reperfusion period in the RtVNX group. However, in the atropine group, HR during ischemic and reperfusion periods significantly increased when compared with baseline. PR interval was no significant difference among all groups at the baseline, ischemic, and reperfusion periods (Fig. 2c). In contrast, PR interval in the atropine group significantly decreased PR during ischemic and reperfusion periods when compared with baseline. QRS duration was not significant difference among all groups at the baseline, ischemic, and reperfusion periods (Fig. 2d). QT interval during ischemia and reperfusion was significantly

decreased in all groups (Fig. 3b). Tpe were significantly decreased in all VNS-treated groups, except during ischemic period in RtVNX group and this effect was abolished by atropine (Fig. 3c). Tpe/QT ratio in the I/R group during the ischemic period increased significantly compared with the baseline and atropine significantly increased Tpe/QT ratio during both ischemic and reperfusion periods (Fig. 3d). Interestingly, there was no significant difference in Tpe/QT ratio during the baseline, ischemic, and reperfusion periods in all VNS-treated groups (Fig. 3d).
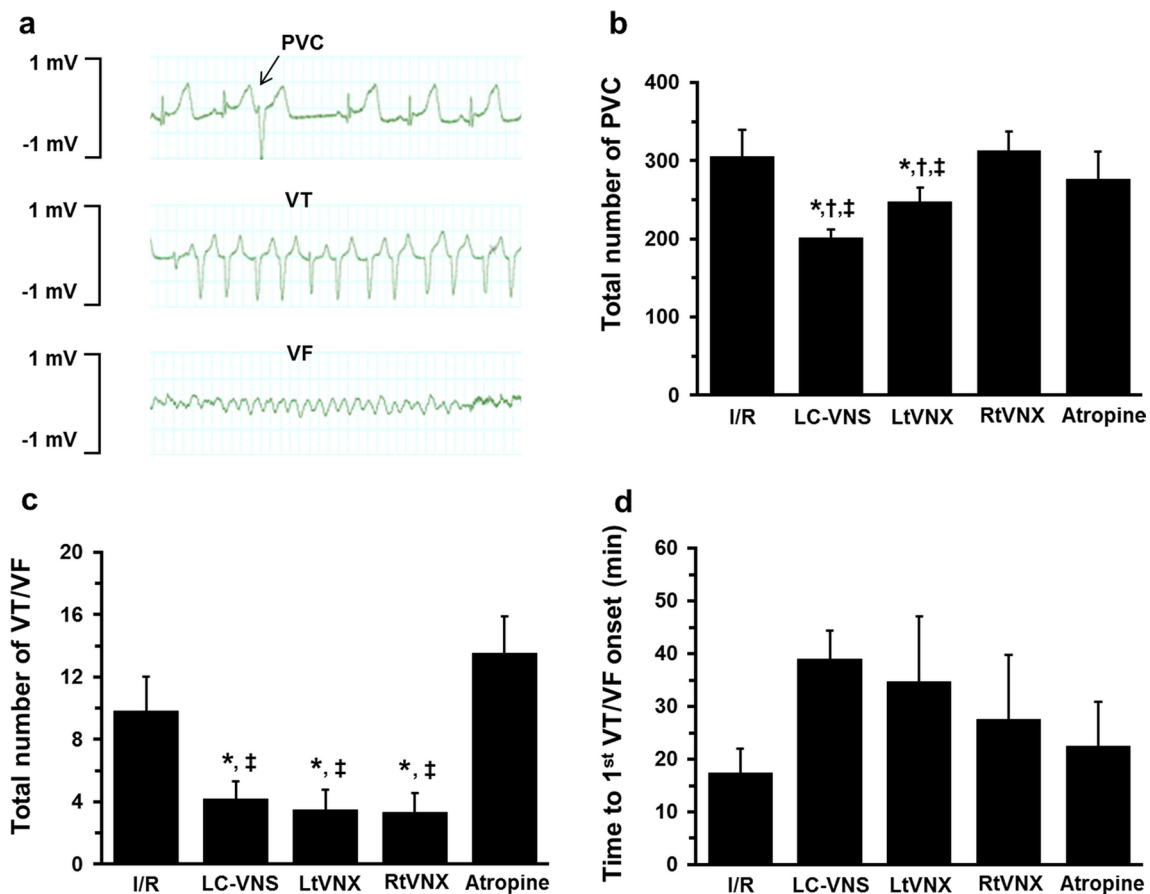
Effects of VNS on the occurrence of cardiac arrhythmia and mortality rate during/after myocardial I/R

Representative tracings of premature ventricular contractions (PVC), ventricular tachycardia (VT), and ventricular fibrillation (VF) have been shown in Fig. 4a. The total number of PVC markedly decreased in both LC-VNS and LtVNX groups, but not RtVNX group, compared with the I/R group (Fig. 4b) The total number of VT/VF episodes was significantly reduced in all VNS-treated groups compared

Fig. 3 The electrocardiographic parameters during the ischemic and the reperfusion periods. **a** Representative of the Tpe interval in LC-VNS group. **b** Effects of VNS on the QT interval. **c** Effects of VNS on the Tpe interval. **d** Effects of VNS on the Tpe/QT ratio. Data are presented as mean ± SE. *$p < 0.05$ vs baseline within group. *I/R* ischemia/reperfusion, *LC-VNS* left cervical vagus nerve stimulation, *LtVNX* left vagus nerve transection, *QT* QT interval, *RtVNX* right vagus nerve transection, *Tpe* T-wave peak to end

Fig. 4 Effects of VNS on the incidence of cardiac arrhythmias. **a** Representative morphology of the PVC, VT and VF. **b** Effects of VNS on the total number of PVC. **c** Effects of VNS on the total number of VT/VF. **d** Effects of VNS on the time to first VT/VF. Data are presented as mean ± SE. *$p < 0.05$ vs I/R group; †$p < 0.05$ vs RtVNX group; ‡$p < 0.05$ vs Atropine group. *I/R* ischemia/reperfusion, *LC-VNS* left cervical vagus nerve stimulation, *LtVNX* left vagus nerve transection, *RtVNX* right vagus nerve transection, *PVC* premature ventricular contraction, *VF* ventricular fibrillation, *VT* ventricular tachycardia

with the I/R group (Fig. 4c). However, time to first VT/VF onset was not significantly different among groups (Fig. 4d). The arrhythmia scores were significantly decreased in both LC-VNS and LtVNX groups compared with the I/R group (Fig. 5a). The mortality rate after I/R induction surgery was significantly lower only in the LC-VNS group compared with the I/R group (Fig. 5b), with all mortality occurring during ischemia or immediately on reperfusion. The effect of VNS on connexin43 phosphorylation at serine 368 has been shown in Fig. 5c. The connexin43 phosphorylation was significantly increased only in the LC-VNS group compared with the I/R group.

Effects of VNS on LV function and myocardial infarct size

The effect of VNS on LV function has been shown in Table 1. In the I/R group, the stroke volume, ejection fraction and stroke work were significantly decreased and the end-diastolic pressure was significantly increased during the ischemic and reperfusion periods compared with the baseline. Interestingly, all VNS-treated groups, the LV functions were preserved during the ischemic and reperfusion periods. The beneficial effects of VNS on LV function were completely abolished by atropine. The percentage of the area at risk (AAR), a percentage of the total ventricular mass, was used to indicate myocardial infarct size. The AAR was not different among groups (I/R 32.8% ± 1.8%; LC-VNS 35.6% ± 2.4%; LtVNX 32.2% ± 1.7%; RtVNX 32.9% ± 0.8%; Atropine 38.1% ± 1.9%; $p > 0.05$) (Fig. 6a). All VNS-treated groups significantly reduced myocardial infarct size compared with the I/R group and this effect was reversed by atropine. Interestingly, the myocardial infarct size was significantly increased in the RtVNX group when compared with the LC-VNS and the LtVNX groups. In contrast, the infarct sizes were not different between the LC-VNS and the LtVNX groups (I/R 45.7% ± 5.4%; VNS
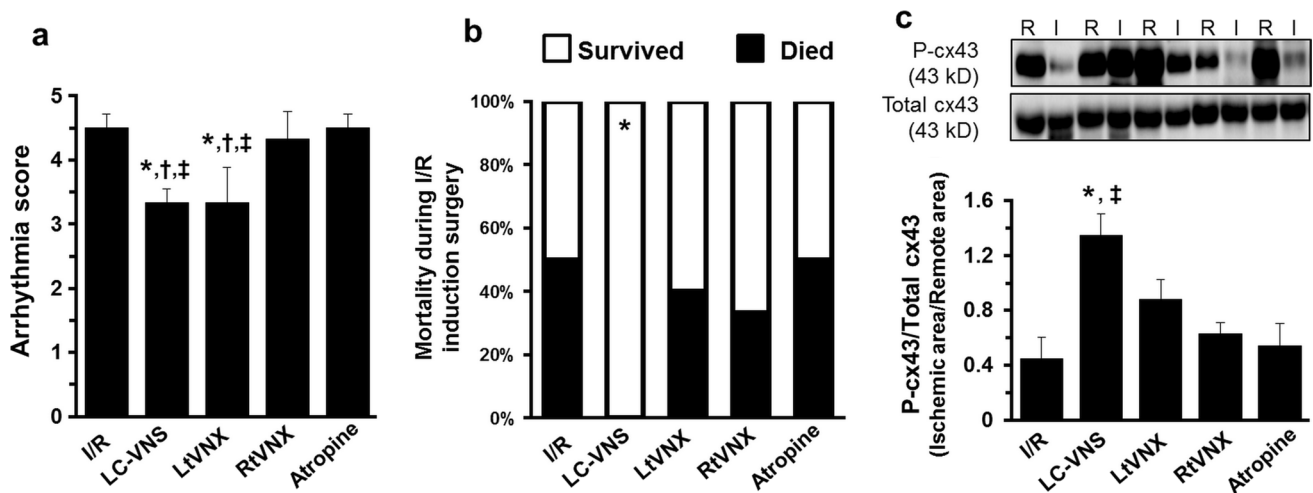
Fig. 5 Effects of VNS on arrhythmia score, percent mortality during I/R induction and myocardial connexin43 expression. **a** Effects of VNS on the arrhythmia score. **b** Percent mortality during I/R induction. **c** Effects of VNS on the phosphorylation of connexin43 at serine 368 in the ischemic myocardium. Data are presented as mean ± SE.

$*p < 0.05$ vs I/R group; $^{†}p < 0.05$ vs RtVNX group; $^{‡}p < 0.05$ vs Atropine group. *I/R* ischemia/reperfusion, *LC-VNS* left cervical vagus nerve stimulation, *LtVNX* left vagus nerve transection, *RtVNX* right vagus nerve transection, *PVC* premature ventricular contraction, *VF* ventricular fibrillation, *VT* ventricular tachycardia

$5.1\% \pm 1.3\%$; LtVNX $7.1\% \pm 1.8\%$; RtVNX $17.6\% \pm 1.4\%$; Atropine $52.9\% \pm 3.5\%$; $p < 0.05$) (Fig. 6b).

Effects of VNS on cardiomyocyte apoptosis

TUNEL staining was performed to detect cardiomyocyte apoptosis. TUNEL positive cells, reported as the percentage of total nuclei, were significantly increased in ischemic area when compared with remote area in the I/R injury group. In contrast, TUNEL positive cells were significantly decreased in all VNS-treated groups and this effect was reversed by atropine (Fig. 6c, d, and Supplemental Fig. S1). Interestingly, % TUNEL positive cell was significantly increased in the RtVNX group when compared with the LC-VNS and the LtVNX groups. In contrast, % TUNEL positive cell was not different between the LC-VNS and the LtVNX groups (Fig. 6c, d, and Supplemental Fig. S1). Additionally, the mechanism underlying the anti-infarct effect of VNS was determined by measuring the key apoptotic markers (Fig. 7). The expression of Bax and the Cleaved caspase-3/Pro caspase-3 ratio was significantly decreased in the VNS-treated groups. However, the levels of Bcl-2 were significantly increased in the LC-VNS and the LtVNX groups, but not in the RtVNX, compared with the I/R group. The administration of atropine totally abolished the anti-apoptotic effects of VNS.

Effects of VNS on oxidative stress activity (MDA) and inflammation

The changes of MDA levels in myocardium between ischemic and remote areas have been shown in Fig. 8a. VNS

significantly decreased the level of MDA in the myocardium compared with the I/R group. However, there was a statistical difference between the RtVNX group compared with the LC-VNS and LtVNX groups. This effect was abolished by atropine. Figure 8b shows the changes of TNF-α levels in myocardium between ischemic and remote areas. Only the LC-VNS group significantly decreased the levels of TNF-α in the myocardium compared with the I/R group. There was no statistically significant difference among the groups with respect to the IL-10 levels (Fig. 8c).

Effects of VNS on mitochondrial function

All VNS-treated groups significantly decreased mitochondrial ROS production (Fig. 9a) and prevented mitochondrial membrane depolarization (Fig. 9b). However, only LC-VNS and LtVNX groups could prevent mitochondrial swelling after I/R (Fig. 9c). Electron photomicrographs demonstrated that in the ischemic area of the I/R group, severe mitochondrial damage was observed as demonstrated by marked mitochondrial swelling accompanied by a disruption in membrane integrity (Fig. 9d).

Effects of VNS on cardiac mitochondrial dynamics

The expression level of MFN2, OPA1, and DRP1 proteins was determined to evaluate mitochondrial dynamics (Fig. 10). Both LC-VNS and LtVNX significantly increased the expression of MFN2, OPA1, and the phosphorylation of DRP1 at Ser 637 as well as significantly decreased phosphorylation of DRP1 at Ser 616 compared with the I/R group.

Table 1 Effects of VNS and Atropine on pressure–volume loop-derived functional parameters

Parameter	I/R			LC-VNS			LtVNX			RtVNX			Atropine		
	Baseline	Ischemia	Reperfusion	Baseline	Ischemia	Reperfusion	Baseline	Ischemia	Reperfusion	Baseline	Ischemia	Reperfusion	Baseline	Ischemia	Reperfusion
SV (ml)	27±3	16±3*	14±3*	26±1	25±3	26±3	29±4	32±5	20±3	34±7	37±5	39±6	26±1	15±1*	15±1*
EF (%)	49±5	28±5*	38±3*	49±4	46±3	49±7	40±4	41±5	44±3	42±7	39±7	43±6	48±3	33±3*	36±2*
ESP (mmHg)	83±6	75±6	86±7	82±9	70±4	65±4	65±3	64±3	67±2	69±3	65±2	62±3	77±4	71±6	74±3
EDP (mmHg)	9±2	18±3*	21±5*	11±3	14±4	13±2	16±2	20±3	21±2	11±1	13±2	11±2	10±1	18±1*	18±2*
SW (mmHg ml)	2126±188	906±259*	879±267*	1811±168	1824±298	1744±285	1883±285	2176±285	1667±504	2019±381	1319±297	1288±210	1687±218	941±120*	1035±134*

Summary of left ventricular (LV) functional parameters at baseline, at 5 min before the end of ischemia, and at 5 min before end of reperfusion (n=6 per group). Values are presented as mean±SE

EDP end-diastolic pressure, EF ejection fraction, ESP end-systolic pressure, I/R ischemia/reperfusion, LC-VNS left cervical vagus nerve stimulation, LtVNX left vagus nerve transection, RtVNX right vagus nerve transection, RtVNX right vagus nerve transection, SV stroke volume, SW stroke work

*p < 0.05 vs baseline within group

The RtVNX significantly increased OPA1 but not MFN2 and phosphorylation of DRP1 at Ser 637 compared with I/R group. In addition, the RtVNX significantly decreased phosphorylation of DRP1 at Ser 616 compared with the I/R group. The effects of VNS on cardiac mitochondrial dynamics were abolished by atropine.

Effects of VNS on cardiac mitochondrial biogenesis and fatty acid oxidation

The biogenesis of the cardiac mitochondria and fatty acid oxidation were studied by determining the key markers for cellular energy metabolism and fatty acid oxidation (AMPK phosphorylation, PGC1α and CPT1) (Fig. 11). Both LC-VNS and LtVNX significantly increased the expression of AMPK phosphorylation, PGC1α and CPT1 compared with the I/R group. However, there was no statistically significant difference in AMPK phosphorylation and PGC1α levels in the RtVNX group. These effects were abolished by atropine.

Effects of VNS on cardiac mitochondrial oxidative phosphorylation

The expressions of cardiac mitochondrial complex I, III and IV were significantly increased in all VNS-treated groups when compared with the I/R group (Fig. 12b, d, e). However, the level of cardiac mitochondrial complex II was significantly increased only in the LC-VNS when compared with the I/R group (Fig. 12c). The level of mitochondrial complex V was not significantly different in all groups (Fig. 12f). These effects were abolished by atropine.

Discussion

In this present study, we sought to investigate whether the cardioprotective effects against myocardial I/R injury of VNS were mainly due to direct ipsilateral efferent vagal fibers activation or indirect effects mediated by the afferent vagal fibers using myocardial infarct size as the primary endpoint. Furthermore, roles of the contralateral efferent vagal fibers during VNS were also investigated. The major findings of this study are as followed: (1) VNS-exerted cardioprotection against myocardial I/R injury via attenuation of mitochondrial dysfunction, improved mitochondrial dynamics and shifted cardiac fatty acid metabolism toward beta oxidation; (2) LC-VNS and LtVNX produced more profound cardioprotection, particularly infarct size reduction, decreased arrhythmia score, oxidative stress and apoptosis and attenuated mitochondrial dysfunction compared to RtVNX; (3) VNS required both ipsilateral and contralateral efferent vagal activities to fully provide its cardioprotection.
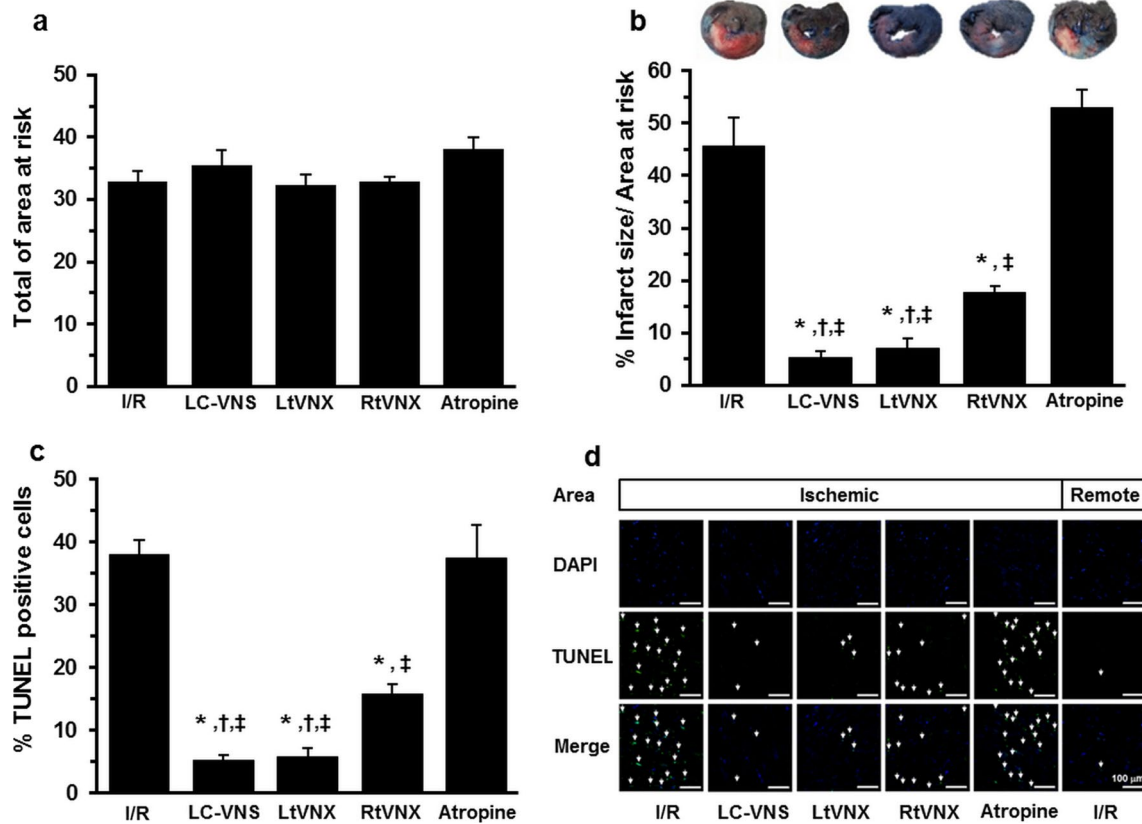
Fig. 6 Effects of VNS on infarct size and the TUNEL positive cells. **a** The total of area at risk. **b** Effects of VNS on the myocardial infarct size per the area at risk (AAR). The inset shows representative photographs obtained after Evan Blue and triphenyltetrazolium chloride staining. Blue indicates the non-threatened myocardium, red indicates the non-infarcted area within the AAR, and white indicates myocardial infarction. **c** Effects of VNS on the TUNEL positive cells. **d** Representative TUNEL assay. Arrow head represented TUNEL positive cell. Data are presented as mean $\pm$ SE. $*p < 0.05$ vs I/R group; $^{\dagger}p < 0.05$ vs RtVNX group. $^{\ddagger}p < 0.05$ vs Atropine group. *I/R* ischemia/reperfusion, *LC-VNS* left cervical vagus nerve stimulation, *LtVNX* left vagus nerve transection, *RtVNX* right vagus nerve transection

These findings suggest that selective efferent VNS may potentially be effective in attenuating myocardial I/R injury.

Impact of VNS during intact, after ipsilateral and contralateral vagus nerve transection on reperfusion arrhythmia and myocardial infarct size

Since both reperfusion arrhythmia [7] and infarct size [39] are the potential serious complications after myocardial reperfusion, strategies to limit these two components of I/R injury have significant therapeutic potential. In the present study, we found that LC-VNS prevented cardiac arrhythmias during I/R as indicated by decreasing the total number of PVC, VT/VF incidence, arrhythmia score, Tpe and preserving Tpe/QT ratio, suggesting that LC-VNS decreased heterogeneity of ventricular repolarization. It is well recognized that increased myocardial infarct size and decreased phosphorylation of connexin43 play an important role in the development of cardiac arrhythmias, including VT/VF,

during I/R [2]. Thus, the anti-arrhythmic effects of VNS might be due to its potential to decrease the arrhythmogenic substrates during I/R by reducing myocardial infarct size and increasing the phosphorylation of connexin43 at the serine 368 residue. In the present study, we found that VNS significantly reduced myocardial infarct size and increased phosphorylation of connexin43 compared with the I/R group, which are consistent with our previous studies in swine model [46] and other studies in rat model [2, 54]. Furthermore, LC-VNS also preserved LV function in the heart subjected to I/R injury when compared with baseline, which might be due to its ability to reduce myocardial infarct size. Because the vagal trunk consists primarily of afferent fibers (80%) [61], the role of these fibers, particularly during VNS, needs to be clearly assessed. Previous study reported that vagal afferent fibers are activated during VNS and decrease efferent parasympathetic electrophysiological and hemodynamic effects of electrical stimulation [56]. However, it is still remained unclear whether the cardioprotection against myocardial I/R injury of VNS is mainly due
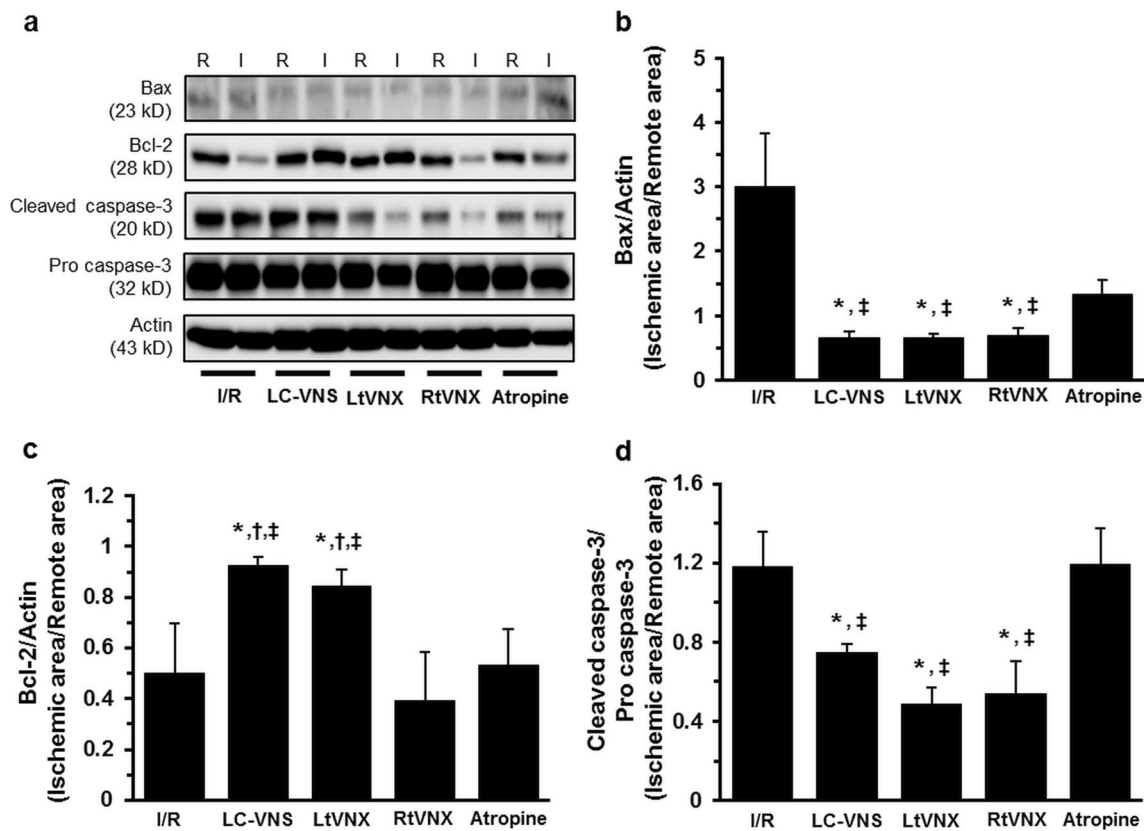
Fig. 7 Effects of VNS on cardiomyocyte apoptosis. **a** Representative bands for Bax, Bcl-2, cleaved caspase-3 and pro-caspase-3. Actin was used as a loading control. **b**, **c** Western blot analysis of Bax and Bcl-2. **d** The ratio between cleaved caspase-3 and pro-caspase-3 expression. Data are presented as mean ± SE. *$p < 0.05$ vs I/R group; †$p < 0.05$ vs RtVNX group; ‡$p < 0.05$ vs Atropine group. *I/R* ischemia/reperfusion, *LC-VNS* left cervical vagus nerve stimulation, *LtVNX* left vagus nerve transection, *RtVNX* right vagus nerve transection
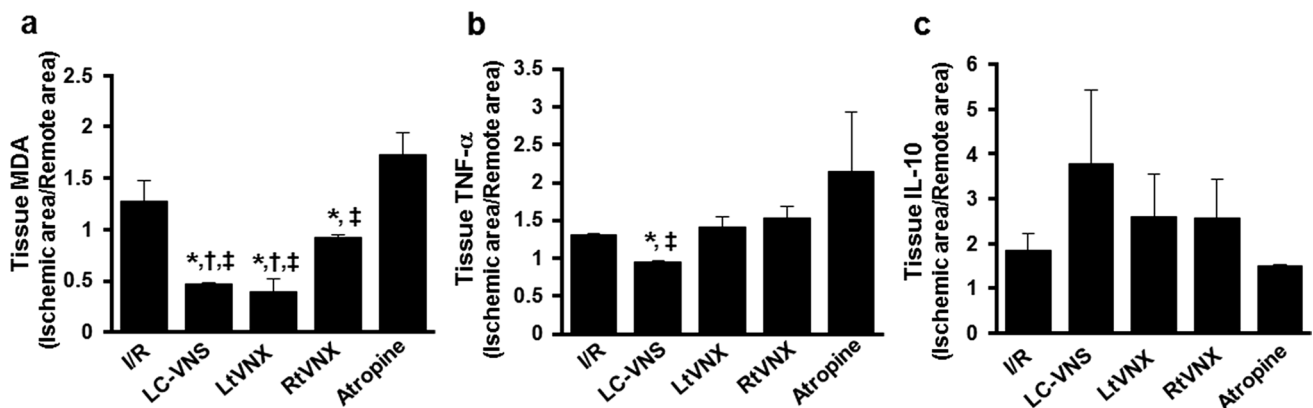

Fig. 8 Effects of VNS on oxidative stress biomarker in myocardium. **a** Myocardium MDA ratios between ischemic and remote areas. **b** Myocardium TNF-α ratios between ischemic and remote areas. **c** Myocardium IL-10 ratios between ischemic and remote areas. Data are presented as mean ± SE. *$p < 0.05$ vs I/R group; †$p < 0.05$ vs RtVNX group; ‡$p < 0.05$ vs Atropine group. *I/R* ischemia/reperfusion, *LC-VNS* left cervical vagus nerve stimulation, *LtVNX* left vagus nerve transection, *RtVNX* right vagus nerve transection

to direct vagal activation through its ipsilateral efferent vagal fibers (motor) or indirect effects mediated by the afferent vagal fibers (sensory). Thus, roles of the ipsilateral afferent vagal fibers during VNS were also investigated by LtVNX

2 cm above the stimulation probe. Interestingly, we found that LtVNX exerted the anti-infarct and anti-arrhythmic effects similar to LC-VNS, suggesting that the anti-infarct effect of VNS was driven primarily through its efferent vagal
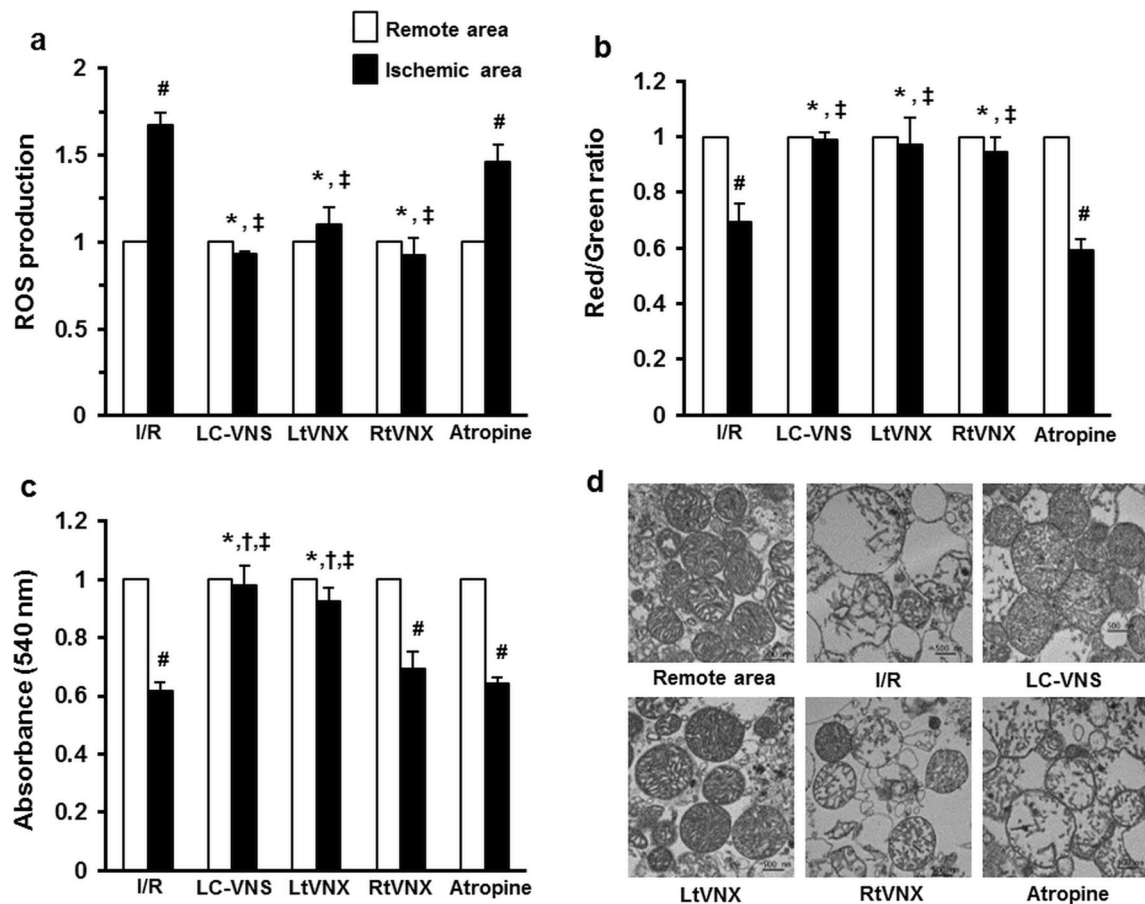
Fig. 9 Effects of VNS on cardiac mitochondria function and morphology. **a** Mitochondrial ROS production. **b** Mitochondrial membrane depolarization. **c** Mitochondrial swelling. **d** Representative electron photomicrographs of a cardiac mitochondrial ultrastructure. Data are prese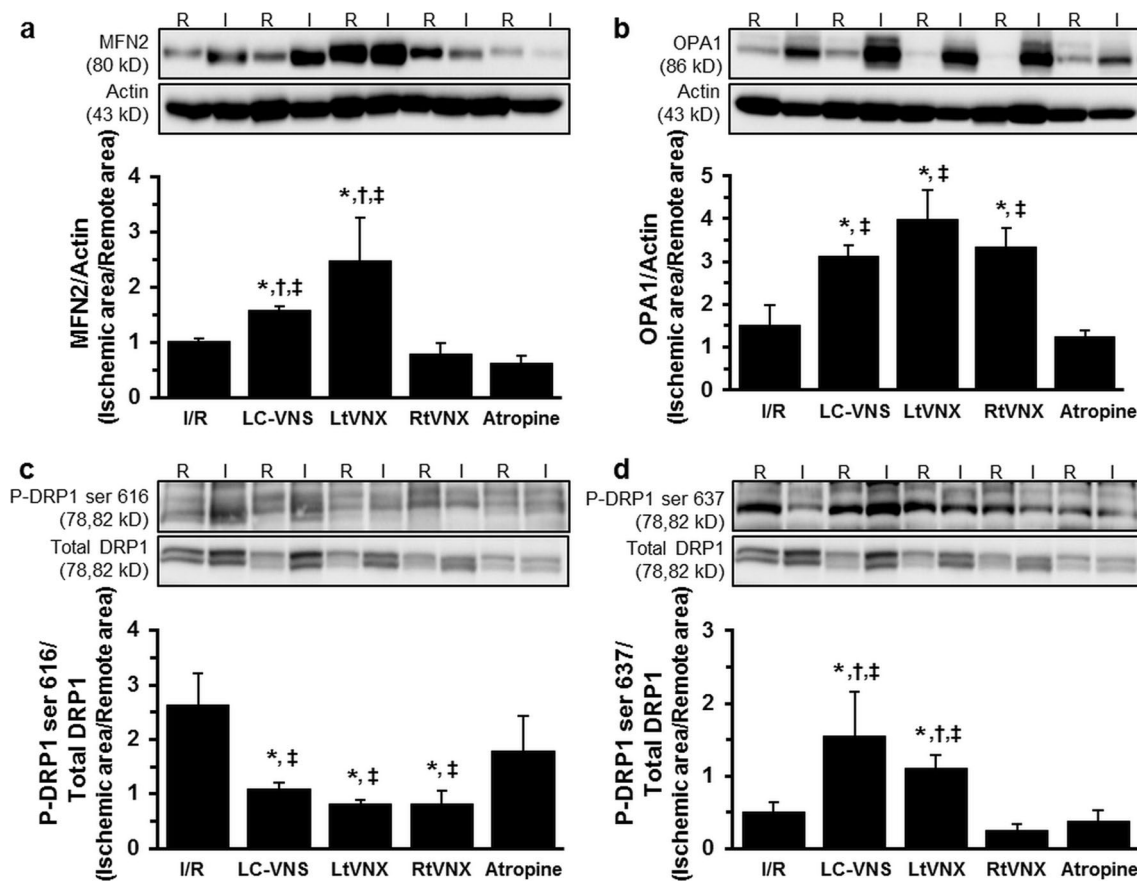nted as mean $\pm$ SE. $^{\#}p < 0.05$ vs remote area within group; $^{*}p < 0.05$ vs I/R group; $^{\dagger}p < 0.05$ vs RtVNX group; $^{\ddagger}p < 0.05$ vs Atropine group. *I/R* ischemia/reperfusion, *LC-VNS* left cervical vagus nerve stimulation, *LtVNX* left vagus nerve transection, *RtVNX* right vagus nerve transection

fibers, rather than the indirect afferent vagal activation in the ipsilateral vagal trunk.

Although all VNS-treated groups exerted cardioprotection against myocardial I/R injury, LC-VNS and LtVNX produced more profound cardioprotection, particularly infarct size reduction (by 89% for LC-VNS and 84% for LtVNX), compared to RtVNX (by 63% reduction). Moreover, for the anti-arrhythmic effect, RtVNX did not significantly decrease the total number of PVC and arrhythmia score, but significantly decreased VT/VF incidence when compared with I/R and atropine groups. Interestingly, RtVNX also preserved LV function similar to the LC-VNS and LtVNX groups. These beneficial effects of VNS were abolished by atropine. Previous study demonstrated that bilateral cervical or subdiaphragmatic vagotomy can also abolish the infarct size reduction by remote ischemic conditioning with one cycle of ischemia (15 min) and reperfusion (10 min) on both hind limbs in rats [4], suggesting the important role of efferent vagal tone to the heart. Moreover, VNS can mimic the effect

of remote ischemic conditioning in rabbits [23] and pigs [51] and reduced infarct size. Interestingly, a previous study using an optogenetic approach to recruit vagal efferent fibers clearly demonstrated that stimulation of vagal efferent-exerted cardioprotection against I/R injury [36]. Thus, these findings suggest that selective efferent VNS may potentially be effective in attenuating myocardial I/R injury partly through mimicking the effect of remote ischemic conditioning [27, 30]. Moreover, our finding also suggested that VNS required the contralateral efferent vagal activities to fully provide its cardioprotection. A recent study in an in vivo rat model of acute myocardial I/R injury demonstrated that infarct size and serum cTnI and CK-MB levels were markedly lower in the combined vagal stimulation perconditioning (VSPerC) and limb remote ischemic perconditioning (LRIPerC) group compared to the use of either treatment alone [52], which indicated that the combination of the two interventions significantly improved cardioprotection compared to the use of either treatment alone.

Fig. 10 Effects of VNS on cardiac mitochondrial dynamics. **a–d** Representative immunoblots (top) and densitometric analysis (bottom) of the mitochondrial dynamic proteins (OPA1, MFN2, P-DRP1 at Ser 616 and Ser 637). Data are presented as mean ± SE. *$p < 0.05$ vs I/R group; †$p < 0.05$ vs RtVNX group; ‡$p < 0.05$ vs Atropine group. *I/R* ischemia/reperfusion, *LC-VNS* left cervical vagus nerve stimulation, *LtVNX* left vagus nerve transection, *RtVNX* right vagus nerve transection

Impact of VNS during intact, after ipsilateral and contralateral vagus nerve transection on myocardial apoptosis during I/R

In the present study, we found that all VNS-treated groups markedly decreased the expression of Bax (a pro-apoptotic protein), Cleaved caspase-3/Pro caspase-3 ratio, and % TUNEL positive cells. However, only LC-VNS and LtVNX significantly increased the expression of Bcl-2 (an anti-apoptotic protein) when compared with other groups. Moreover, % TUNEL positive cell of RtVNX significantly increased when compared with LC-VNS (both intact and LtVNX), which also consistent with myocardial infract size. Myocardial I/R injury leads to the activation of program cell deaths, including cell apoptosis and necrosis [53]. Specifically, the decrease in an anti-apoptosis Bcl-2 and the increase in a pro-apoptosis Bax expression are the underling of myocardial ischemia-induced apoptosis [29]. Moreover, a recent study demonstrated that overexpression of cardiac specific caspase 3, a key molecule in the execution of apoptosis, decreased cardiac function and caused abnormality of ultrastructural

damage to the nucleus as measured by the TUNEL-staining method [33]. These results suggested that the anti-apoptosis Bcl-2 molecule could be responsible for the reduction of % TUNEL positive cells observed in both LC-VNS and LtVNX groups. Previous study in rat model demonstrated that VNS prevents downregulation of the anti-apoptotic protein Bcl-2 [29], which consistent with our finding. Thus, our results suggested that VNS reduced myocardial infarct size through the anti-apoptotic effect. Moreover, VNS also required the contralateral efferent vagal activities to fully provide its cardioprotection.

Impact of VNS during intact, after ipsilateral and contralateral vagus nerve transection on cardiac mitochondrial function and inflammation during I/R

Furthermore, accumulating evidence has demonstrated that myocardial ischemia and post-ischemic reperfusion cause a wide array of functional and structural alterations of cardiac mitochondria [6, 9, 21, 46, 47]. Our previous studies
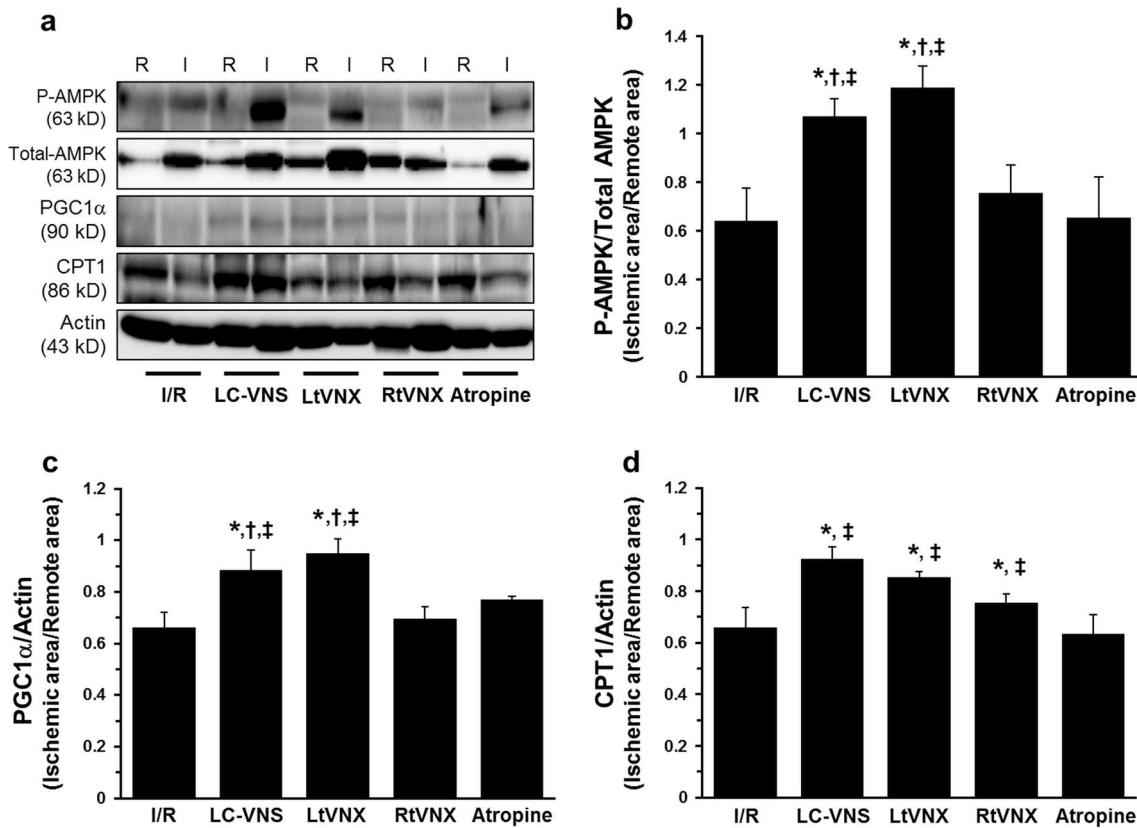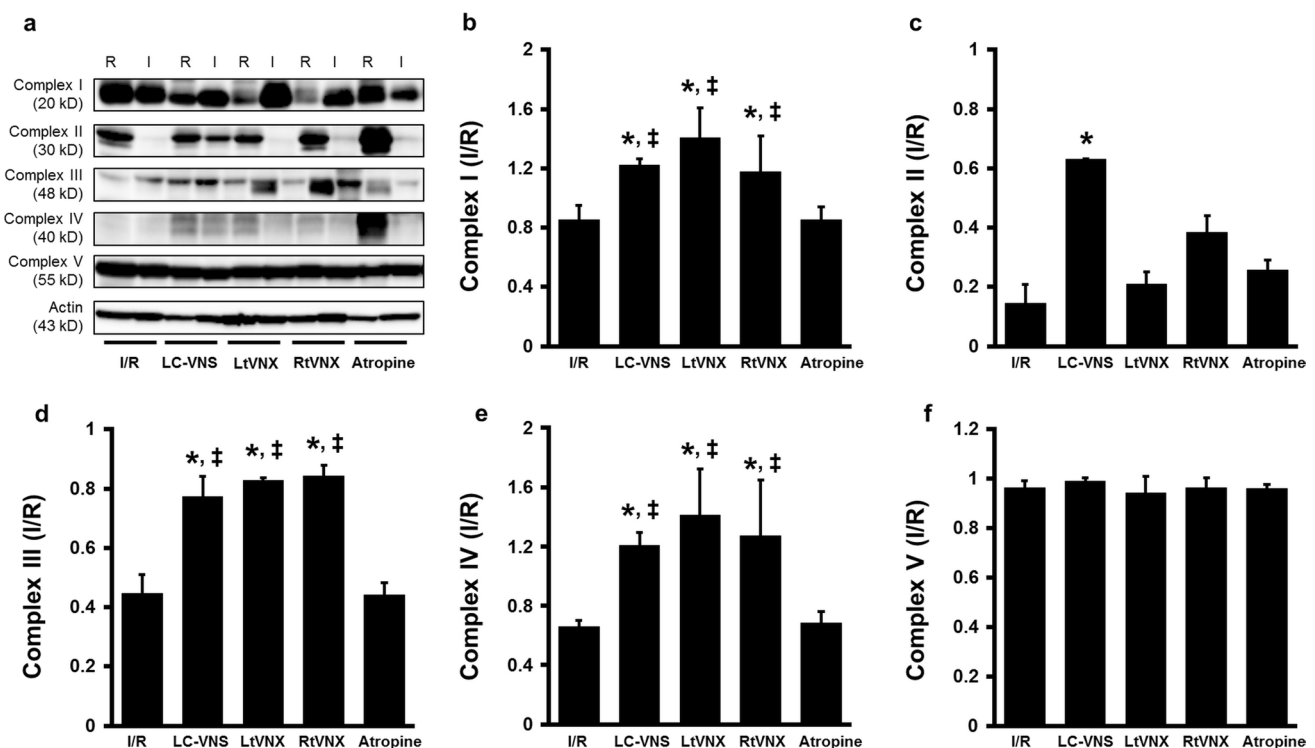
Fig. 11 Effects of VNS on proteins related to cardiac metabolism. **a** Representative immunoblots of key proteins involved in cardiac metabolism. **b** Quantitative analysis of AMPK phosphorylation in the ischemic area normalized with that in the remote area, $n = 6$/group. **c** Myocardial PGC1α expression in the ischemic area normalized with that in the remote area, $n = 6$/group. **d** Cardiac mitochondrial CPT1 expression in the ischemic area normalized with that in the remote area, $n = 6$/group. Data are presented as mean ± SE. *$p < 0.05$ vs I/R group; [†]$p < 0.05$ vs RtVNX group; [‡]$p < 0.05$ vs Atropine group. *I/R* ischemia/reperfusion, *LC-VNS* left cervical vagus nerve stimulation, *LtVNX* left vagus nerve transection, *RtVNX* right vagus nerve transection

have shown that one potential possible mechanism underlying the pronounced cardioprotection of VNS against I/R injury is through the prevention of cardiac mitochondrial dysfunction [46, 47]. Increasing the ROS production and the oscillation of mitochondrial membrane potential have been shown to play an important role in the genesis of cardiac arrhythmias and myocardial infarction [9]. In the present study, all VNS-treated groups significantly reduced cardiac mitochondrial ROS production and prevented depolarization of mitochondrial membrane potential. These results could be responsible for the anti-infarct, anti-arrhythmia and the preservation of cardiac function of VNS in the heart subjected to myocardial I/R. Interestingly, we found that both LC-VNS and LtVNX, but not RtVNX, could prevent mitochondrial swelling after I/R injury. This result might explain why LC-VNS and LtVNX have higher efficiency on infarct size and prevention of cardiac arrhythmia than RtVNX.

In addition to cardiac mitochondrial dysfunction during I/R, inflammatory processes have been shown to play a critical role during myocardial I/R injury [35]. In the present study, only LC-VNS significantly decreased the expression level of myocardial TNF-α (a pro-inflammation marker) after I/R injury. However, the level of tissue TNF-α was not changed after vagus nerve transection, suggesting that VNS required both ipsilateral and contralateral efferent vagal activities to fully exert the anti-inflammation. Thus, it is reasonable to speculate that LC-VNS, both efferent vagal fibers are intact, provides the vagal tone that high enough to reach the activation threshold of the anti-inflammatory signaling pathway. However, the expression level of myocardial IL-10 (anti-inflammation) tended to increase in all VNS treatments after I/R injury, but did not reach the statistically significant level. Additionally, both LC-VNS and LtVNX significantly decreased the oxidative stress level as shown by the reduction in myocardial MDA levels after I/R when compared with RtVNX and atropine groups. Again, this result suggests that both efferent vagal fibers are required for VNS to provide the vagal tone that high enough to reach the activation threshold of the anti-oxidative effect.

Fig. 12 The effects of VNS on proteins related to cardiac mitochondrial oxidative phosphorylation in pigs with cardiac I/R injury. **a** Representative Western blot bands of cardiac mitochondrial complexes I, II, III, IV and V in the ischemic area and the remote area. **b** Cardiac mitochondrial complex I expression in the ischemic area normalized with that in the remote area, $n = 6$/group. **c** Cardiac mitochondrial complex II expression in the ischemic area normalized with that in the remote area, $n = 6$/group. **d** Cardiac mitochondrial complex III expression in the ischemic area normalized with that in the remote area, $n = 6$/group. **e** Cardiac mitochondrial complex IV expression in the ischemic area normalized with that in the remote area, $n = 6$/group. **f** Cardiac mitochondrial complex V expression in the ischemic area normalized with that in the remote area, $n = 6$/group. Data are presented as mean ± SE. *$p < 0.05$ vs I/R group; †$p < 0.05$ vs RtVNX group; ‡$p < 0.05$ vs Atropine group. *I/R* ischemia/reperfusion, *LC-VNS* left cervical vagus nerve stimulation, *LtVNX* left vagus nerve transection, *RtVNX* right vagus nerve transection

Impact of VNS during intact, after ipsilateral and contralateral vagus nerve transection on cardiac myocardial dynamics and fatty acid oxidation during I/R

Mitochondria are dynamic organelles that continually undergo fusion and fission [11, 12, 33, 55, 66]. Generally, mitochondrial outer and inner membrane fusion events are mediated by MFN1/2 and OPA1 protein [13]. In contrast, phosphorylation of DRP1 on Ser 616 promotes mitochondrial fission and phosphorylation of DRP1 on Ser 637 inhibits mitochondrial fission [12]. A growing body of literature has shown that enhancing mitochondrial dynamics and reducing mitochondrial oxidative stress have emerged as crucial therapeutic strategies to ameliorate myocardial I/R injury [48, 57]. In the present study, LC-VNS and LtVNX, but not RtVNX, significantly increased mitochondrial fusion protein (MFN2 and OPA1) expression, increased phosphorylation of DRP1 on Ser 637, and decreased the phosphorylation of DRP1 on Ser 616 when compared with I/R group.

Additionally, previous studies demonstrated that AMPK activation played an important role in ACh-mediated cell survival via an AMPK-induced cardiomyocyte autophagy pathway during cardiomyocyte hypoxia/reoxygenation injury [64]. Interestingly, AMPK activation can prevent mitochondrial fission by decreasing DRP1 and Fis1 levels in high glucose-induced endothelial apoptosis [5]. In the present study, LC-VNS and LtVNX, but not RtVNX, significantly increased the phosphorylation of AMPK when compared with I/R group, suggesting that AMPK was indeed involved in VNS-mediated protection of mitochondrial dynamics and function. Furthermore, it has been shown that pathological stressors for the heart, such as ischemia, are associated with a downregulation of mitochondrial biogenesis via PGC1α activity [1], and the impairment of the PGC1α-mediated mitochondrial biogenesis increased heart vulnerability to myocardial I/R injury [57]. Accordingly, upregulation of the PGC1α pathway has been shown to confer protection against simulated I/R in cardiomyoblast cells [48]. Previous studies in skeletal muscle have demonstrated

that pharmacological- or exercise-induced AMPK activation increased PGC1α to promote mitochondrial biogenesis [3, 49, 65]. In the present study, LC-VNS and LtVNX, but not RtVNX, significantly increased the expression level of AMPK phosphorylation and PGC1α. Moreover, VNS significantly increased CPT1 expression in the heart subjected to I/R injury and this effect was abolished after administration of atropine, suggesting that VNS exerts its cardioprotection against I/R injury through muscarinic receptors (mAChR). At cellular level, acetylcholine (ACh), a neurotransmitter of the cardiac vagus nerve has been shown to replicate the effect of cardiac ischemic conditioning, a therapeutic strategy for protecting organs or tissue against the detrimental effects of myocardial I/R injury. ACh, a non-selective ligand, initiates its downstream signal by activating G-protein-coupled mAChR or by binding to nicotinic receptors (nAChR) that are ligand-gated ion channels, and both receptors are present in the heart [24, 32, 38]. Interestingly, previous study demonstrated that both mAChR and nAChR significantly increased after I/R, suggesting the compensatory response to myocardial I/R injury [38]. Although the effects of ACh on both electrical and mechanical properties of the heart are well known and have been attributed to mAChRs activation, including our present study, the effects of the action of ACh on α7nAChRs cannot be excluded. In an isolated perfused rat heart, GTS21 (α7nAChR agonist) administration at the initiation of reperfusion provided therapeutic benefit by improving cardiac contractile function through stimulating prosurvival signaling pathways, leading to the preservation of mitochondrial function, maintaining intracellular ATP and reducing ROS production, thus limiting infarct size [38]. Moreover, during ischemia, VNS exhibited a significant reduction in the number of apoptotic cells [10]. Interestingly, this beneficial effect was abrogated by mecamylamine (MEC), a non-selective α7nAChR antagonist [10]. Additionally, VNS has been shown to protect against remote vascular dysfunction, through the cholinergic anti-inflammatory pathway which is dependent on α7nAChR [63]. These findings suggest that not only the activation of the mAChRs, but the activation of α7nAChRs can also trigger cardioprotective signaling cascades which are effective against I/R injury. Thus, the distinct role of mAChR versus nAChR on these mechanisms in the heart remains to be determined.

The observed elevation of AMPK phosphorylation, PGC1α and CPT1 expression suggests that cardiac fatty acid metabolism is shifted toward mitochondrial beta oxidation. Furthermore, increased levels of cardiac mitochondrial complexes I, II (only in the LC-VNS), III and IV of the electron transport chain were significantly increased in VNS-treated groups. Therefore, increased levels of cardiac mitochondrial complexes by VNS may also be responsible for the preservation of cardiac function in the heart subjected to I/R injury. In summary, we have demonstrated that

the mechanism underlying the cardioprotection of VNS was associated with anti-apoptosis, anti-oxidative stress, anti-inflammation, prevent cardiac mitochondrial dysfunction, improved mitochondrial dynamic (increased mitochondrial fusion and decreased mitochondrial fission), improved mitochondrial biogenesis, shifted cardiac fatty acid metabolism toward beta oxidation and increased levels of cardiac mitochondrial complexes. Finally, VNS required both ipsilateral and contralateral efferent vagal activities to fully provide its cardioprotection against myocardial I/R injury, suggesting the important role of maintaining cardiac vagal tone during I/R (Supplemental Fig. S2).

Conclusions and clinical implications

Our study has shown that VNS-exerted cardioprotection against myocardial I/R injury via attenuation of mitochondrial dysfunction, increased mitochondrial fusion, decreased mitochondrial fission and shifted cardiac fatty acid metabolism toward beta oxidation. However, LC-VNS and LtVNX produced more profound cardioprotection, particularly infarct size reduction, decreased arrhythmia score and apoptosis and attenuated mitochondrial dysfunction compared to RtVNX. Our findings suggest that selective efferent VNS may potentially be effective in attenuating myocardial I/R injury. Moreover, VNS also required the contralateral efferent vagal activities to fully provide its cardioprotection. It is important to note that most of the current devices implanted in animal and clinical investigations, activate both afferent and efferent pathways [20, 22, 25, 34, 42, 60, 62]. Recently, Patel and colleagues have developed a kilohertz electrical stimulation (KES) nerve block technique to preferentially activate efferent pathways while blocking afferent pathways without the need to transect the vagus nerve [41]. Thus, using KES nerve block that selectively stimulates the efferent vagal nerve fibers, VNS may potentially be an attractive potential adjuvant therapy to limit reperfusion injury in patients with acute MI. However, further clinical studies are needed before we can conclude that VNS is a viable clinical treatment in the affected MI patients.

Compliance with ethical standards

Conflict of interest The authors declare that there are no conflicts of interest associated with this study.

References

1. Ahuja P, Zhao P, Angelis E, Ruan H, Korge P, Olson A, Wang Y, Jin ES, Jeffrey FM, Portman M, Maclellan WR (2010) Myc controls transcriptional regulation of cardiac metabolism and mitochondrial biogenesis in response to pathological stress in mice. J Clin Invest 120:1494–1505. https://doi.org/10.1172/jci38331

2. Ando M, Katare RG, Kakinuma Y, Zhang D, Yamasaki F, Muramoto K, Sato T (2005) Efferent vagal nerve stimulation protects heart against ischemia-induced arrhythmias by preserving connexin43 protein. Circulation 112:164–170. https://doi.org/10.1161/circulationaha.104.525493

3. Atherton PJ, Babraj J, Smith K, Singh J, Rennie MJ, Wackerhage H (2005) Selective activation of AMPK-PGC-1alpha or PKB-TSC2-mTOR signaling can explain specific adaptive responses to endurance or resistance training-like electrical muscle stimulation. Faseb J 19:786–788. https://doi.org/10.1096/fj.04-2179fje

4. Basalay MV, Mastitskaya S, Mrochek A, Ackland GL, del Arroyo AG, Sanchez J, Sjoquist P-O, Pernow J, Gourine AV, Gourine A (2016) Glucagon-like peptide-1 (GLP-1) mediates cardioprotection by remote ischaemic conditioning. Cardiovasc Res 112:669–676. https://doi.org/10.1093/cvr/cvw216

5. Bhatt MP, Lim Y-C, Kim Y-M, Ha K-S (2013) C-peptide activates AMPKα and prevents ROS-mediated mitochondrial fission and endothelial apoptosis in diabetes. Diabetes 62:3851–3862. https://doi.org/10.2337/db13-0039

6. Boengler K, Ruiz-Meana M, Gent S, Ungefug E, Soetkamp D, Miro-Casas E, Cabestrero A, Fernandez-Sanz C, Semenzato M, Di Lisa F, Rohrbach S, Garcia-Dorado D, Heusch G, Schulz R (2012) Mitochondrial connexin 43 impacts on respiratory complex I activity and mitochondrial oxygen consumption. J Cell Mol Med 16:1649–1655. https://doi.org/10.1111/j.1582-4934.2011.01516.x

7. Brack KE, Winter J, Ng GA (2013) Mechanisms underlying the autonomic modulation of ventricular fibrillation initiation—tentative prophylactic properties of vagus nerve stimulation on malignant arrhythmias in heart failure. Heart Fail Rev 18:389–408. https://doi.org/10.1007/s10741-012-9314-2

8. Brown DA, Aon MA, Akar FG, Liu T, Sorarrain N, O'Rourke B (2008) Effects of 4′-chlorodiazepam on cellular excitation-contraction coupling and ischaemia-reperfusion injury in rabbit heart. Cardiovasc Res 79:141–149. https://doi.org/10.1093/cvr/cvn053

9. Brown DA, O'Rourke B (2010) Cardiac mitochondria and arrhythmias. Cardiovasc Res 88:241–249. https://doi.org/10.1093/cvr/cvq231

10. Calvillo L, Vanoli E, Andreoli E, Besana A, Omodeo E, Gnecchi M, Zerbi P, Vago G, Busca G, Schwartz PJ (2011) Vagal stimulation, through its nicotinic action, limits infarct size and the inflammatory response to myocardial ischemia and reperfusion. J Cardiovasc Pharmacol 58:500–507. https://doi.org/10.1097/FJC.0b013e31822b7204

11. Chan DC (2012) Fusion and fission: interlinked processes critical for mitochondrial health. Annu Rev Genet 46:265–287. https://doi.org/10.1146/annurev-genet-110410-132529

12. Chang CR, Blackstone C (2010) Dynamic regulation of mitochondrial fission through modification of the dynamin-related protein Drp1. Ann N Y Acad Sci 1201:34–39. https://doi.org/10.1111/j.1749-6632.2010.05629.x

13. Chen H, Chan DC (2010) Physiological functions of mitochondrial fusion. Ann N Y Acad Sci 1201:21–25. https://doi.org/10.1111/j.1749-6632.2010.05615.x

14. Chinda K, Palee S, Surinkaew S, Phornphutkul M, Chattipakorn S, Chattipakorn N (2013) Cardioprotective effect of dipeptidyl peptidase-4 inhibitor during ischemia-reperfusion injury. Int J Cardiol 167:451–457. https://doi.org/10.1016/j.ijcard.2012.01.011

15. Chunchai T, Samniang B, Sripetchwandee J, Pintana H, Pongkan W, Kumfu S, Shinlapawittayatorn K, KenKnight BH, Chattipakorn N, Chattipakorn SC (2016) Vagus nerve stimulation exerts the neuroprotective effects in obese-insulin resistant rats, leading to the improvement of cognitive function. Sci Rep 6:26866. https://doi.org/10.1038/srep26866

16. Coote JH (2013) Myths and realities of the cardiac vagus. J Physiol 591:4073–4085. https://doi.org/10.1113/jphysiol.2013.257758

17. Curtis MJ, Hancox JC, Farkas A, Wainwright CL, Stables CL, Saint DA, Clements-Jewery H, Lambiase PD, Billman GE, Janse MJ, Pugsley MK, Ng GA, Roden DM, Camm AJ, Walker MJ (2013) The Lambeth Conventions (II): guidelines for the study of animal and human ventricular and supraventricular arrhythmias. Pharmacol Ther 139:213–248. https://doi.org/10.1016/j.pharmthera.2013.04.008

18. D'Souza A, Bucchi A, Johnsen AB, Logantha SJ, Monfredi O, Yanni J, Prehar S, Hart G, Cartwright E, Wisloff U, Dobrynski H, DiFrancesco D, Morris GM, Boyett MR (2014) Exercise training reduces resting heart rate via downregulation of the funny channel HCN4. Nat Commun 5:3775. https://doi.org/10.1038/ncomms4775

19. Danson EJF, Paterson DJ (2003) Enhanced neuronal nitric oxide synthase expression is central to cardiac vagal phenotype in exercise-trained mice. J Physiol 546:225–232. https://doi.org/10.1113/jphysiol.2002.031781

20. De Ferrari GM, Crijns HJ, Borggrefe M, Milasinovic G, Smid J, Zabel M, Gavazzi A, Sanzo A, Dennert R, Kuschyk J, Raspopovic S, Klein H, Swedberg K, Schwartz PJ (2011) Chronic vagus nerve stimulation: a new and promising therapeutic approach for chronic heart failure. Eur Heart J 32:847–855. https://doi.org/10.1093/eurheartj/ehq391

21. Di Lisa F, Bernardi P (2006) Mitochondria and ischemia-reperfusion injury of the heart: fixing a hole. Cardiovasc Res 70:191–199. https://doi.org/10.1016/j.cardiores.2006.01.016

22. Dicarlo L, Libbus I, Amurthur B, Kenknight BH, Anand IS (2013) Autonomic regulation therapy for the improvement of left ventricular function and heart failure symptoms: the ANTHEM-HF study. J Card Fail 19:655–660. https://doi.org/10.1016/j.cardfail.2013.07.002

23. Donato M, Buchholz B, Rodriguez M, Perez V, Inserte J, Garcia-Dorado D, Gelpi RJ (2013) Role of the parasympathetic nervous system in cardioprotection by remote hindlimb ischaemic preconditioning. Exp Physiol 98:425–434. https://doi.org/10.1113/expphysiol.2012.066217

24. Dvorakova M, Lips KS, Bruggmann D, Slavikova J, Kuncova J, Kummer W (2005) Developmental changes in the expression of nicotinic acetylcholine receptor alpha-subunits in the rat heart. Cell Tissue Res 319:201–209. https://doi.org/10.1007/s00441-004-1008-1

25. Hauptman PJ, Schwartz PJ, Gold MR, Borggrefe M, Van Veldhuisen DJ, Starling RC, Mann DL (2012) Rationale and study design of the increase of vagal tone in heart failure study: INOVATE-HF. Am Heart J 163(954–962):e951. https://doi.org/10.1016/j.ahj.2012.03.021

26. Heusch G (2015) Molecular basis of cardioprotection: signal transduction in ischemic pre-, post-, and remote conditioning. Circ Res 116:674–699. https://doi.org/10.1161/circresaha.116.305348

27. Heusch G (2017) Vagal cardioprotection in reperfused acute myocardial infarction. JACC Cardiovasc Interv 10:1521–1522. https://doi.org/10.1016/j.jcin.2017.05.063

28. Heusch G, Deussen A, Thamer V (1985) Cardiac sympathetic nerve activity and progressive vasoconstriction distal to coronary stenoses: feed-back aggravation of myocardial ischemia. J Auton Nerv Syst 13:311–326. https://doi.org/10.1016/0165-1838(85)90020-7

29. Katare RG, Ando M, Kakinuma Y, Arikawa M, Handa T, Yamasaki F, Sato T (2009) Vagal nerve stimulation prevents reperfusion injury through inhibition of opening of mitochondrial permeability transition pore independent of the bradycardiac effect. J Thorac Cardiovasc Surg 137:223–231. https://doi.org/10.1016/j.jtcvs.2008.08.020

30. Kleinbongard P, Skyschally A, Heusch G (2017) Cardioprotection by remote ischemic conditioning and its signal transduction. Pflugers Arch 469:159–181. https://doi.org/10.1007/s00424-016-1922-6

31. Kong SS, Liu JJ, Yu XJ, Lu Y, Zang WJ (2012) Protection against ischemia-induced oxidative stress conferred by vagal stimulation in the rat heart: involvement of the AMPK-PKC pathway. Int J Mol Sci 13:14311–14325. https://doi.org/10.3390/ijms131114311

32. Li DL, Liu BH, Sun L, Zhao M, He X, Yu XJ, Zang WJ (2010) Alterations of muscarinic acetylcholine receptors-2, 4 and alpha7-nicotinic acetylcholine receptor expression after ischaemia/reperfusion in the rat isolated heart. Clin Exp Pharmacol Physiol 37:1114–1119. https://doi.org/10.1111/j.1440-1681.2010.05448.x

33. Li F, Fan X, Zhang Y, Pang L, Ma X, Song M, Kou J, Yu B (2016) Cardioprotection by combination of three compounds from ShengMai preparations in mice with myocardial ischemia/reperfusion injury through AMPK activation-mediated mitochondrial fission. Sci Rep 6:37114. https://doi.org/10.1038/srep37114

34. Libbus I, Nearing BD, Amurthur B, KenKnight BH, Verrier RL (2016) Autonomic regulation therapy suppresses quantitative T-wave alternans and improves baroreflex sensitivity in patients with heart failure enrolled in the ANTHEM-HF study. Heart Rhythm 13:721–728. https://doi.org/10.1016/j.hrthm.2015.11.030

35. Liu J, Wang H, Li J (2016) Inflammation and inflammatory cells in myocardial infarction and reperfusion injury: a double-edged sword. Clin Med Insights Cardiol 10:79–84. https://doi.org/10.4137/CMC.S33164

36. Mastitskaya S, Marina N, Gourine A, Gilbey MP, Spyer KM, Teschemacher AG, Kasparov S, Trapp S, Ackland GL, Gourine AV (2012) Cardioprotection evoked by remote ischaemic preconditioning is critically dependent on the activity of vagal preganglionic neurones. Cardiovasc Res 95:487–494. https://doi.org/10.1093/cvr/cvs212

37. Mateos R, Lecumberri E, Ramos S, Goya L, Bravo L (2005) Determination of malondialdehyde (MDA) by high-performance liquid chromatography in serum and liver as a biomarker for oxidative stress. Application to a rat model for hypercholesterolemia and evaluation of the effect of diets rich in phenolic antioxidants from fruits. J Chromatogr B Analyt Technol Biomed Life Sci 827:76–82. https://doi.org/10.1016/j.jchromb.2005.06.035

38. Mavropoulos SA, Khan NS, Levy ACJ, Faliks BT, Sison CP, Pavlov VA, Zhang Y, Ojamaa K (2017) Nicotinic acetylcholine receptor-mediated protection of the rat heart exposed to ischemia reperfusion. Mol Med. https://doi.org/10.2119/molmed.2017.00091

39. Miller TD, Christian TF, Hopfenspirger MR, Hodge DO, Gersh BJ, Gibbons RJ (1995) Infarct size after acute myocardial infarction measured by quantitative tomographic 99mTc sestamibi imaging predicts subsequent mortality. Circulation 92:334–341. https://doi.org/10.1161/01.CIR.92.3.334

40. Palee S, Weerateerangkul P, Chinda K, Chattipakorn SC, Chattipakorn N (2013) Mechanisms responsible for beneficial and adverse effects of rosiglitazone in a rat model of acute cardiac ischaemia-reperfusion. Exp Physiol 98:1028–1037. https://doi.org/10.1113/expphysiol.2012.070433

41. Patel YA, Saxena T, Bellamkonda RV, Butera RJ (2017) Kilohertz frequency nerve block enhances anti-inflammatory effects of vagus nerve stimulation. Sci Rep 7:39810. https://doi.org/10.1038/srep39810

42. Premchand RK, Sharma K, Mittal S, Monteiro R, Dixit S, Libbus I, DiCarlo LA, Ardell JL, Rector TS, Amurthur B, KenKnight BH, Anand IS (2014) Autonomic regulation therapy via left or right cervical vagus nerve stimulation in patients with chronic heart failure: results of the ANTHEM-HF trial. J Card Fail 20:808–816. https://doi.org/10.1016/j.cardfail.2014.08.009

43. Ray PD, Huang BW, Tsuji Y (2012) Reactive oxygen species (ROS) homeostasis and redox regulation in cellular signaling. Cell Signal 24:981–990. https://doi.org/10.1016/j.cellsig.2012.01.008

44. Samniang B, Shinlapawittayatorn K, Chunchai T, Pongkan W, Kumfu S, Chattipakorn SC, KenKnight BH, Chattipakorn N (2016) Vagus nerve stimulation improves cardiac function by preventing mitochondrial dysfunction in obese-insulin resistant rats. Sci Rep 6:19749. https://doi.org/10.1038/srep19749

45. Schwartz PJ, De Ferrari GM, Sanzo A, Landolina M, Rordorf R, Raineri C, Campana C, Revera M, Ajmone-Marsan N, Tavazzi L, Odero A (2008) Long term vagal stimulation in patients with advanced heart failure: first experience in man. Eur J Heart Fail 10:884–891. https://doi.org/10.1016/j.ejheart.2008.07.016

46. Shinlapawittayatorn K, Chinda K, Palee S, Surinkaew S, Kumfu S, Kumphune S, Chattipakorn S, KenKnight BH, Chattipakorn N (2014) Vagus nerve stimulation initiated late during ischemia, but not reperfusion, exerts cardioprotection via amelioration of cardiac mitochondrial dysfunction. Heart Rhythm 11:2278–2287. https://doi.org/10.1016/j.hrthm.2014.08.001

47. Shinlapawittayatorn K, Chinda K, Palee S, Surinkaew S, Thunsiri K, Weerateerangkul P, Chattipakorn S, KenKnight BH, Chattipakorn N (2013) Low-amplitude, left vagus nerve stimulation significantly attenuates ventricular dysfunction and infarct size through prevention of mitochondrial dysfunction during acute ischemia-reperfusion injury. Heart Rhythm 10:1700–1707. https://doi.org/10.1016/j.hrthm.2013.08.009

48. Sun L, Zhao M, Yu XJ, Wang H, He X, Liu JK, Zang WJ (2013) Cardioprotection by acetylcholine: a novel mechanism via mitochondrial biogenesis and function involving the PGC-1alpha pathway. J Cell Physiol 228:1238–1248. https://doi.org/10.1002/jcp.24277

49. Terada S, Goto M, Kato M, Kawanaka K, Shimokawa T, Tabata I (2002) Effects of low-intensity prolonged exercise on PGC-1 mRNA expression in rat epitrochlearis muscle. Biochem Biophys Res Commun 296:350–354. https://doi.org/10.1016/S0006-291X(02)00881-1

50. Thummasorn S, Kumfu S, Chattipakorn S, Chattipakorn N (2011) Granulocyte-colony stimulating factor attenuates mitochondrial dysfunction induced by oxidative stress in cardiac mitochondria. Mitochondrion 11:457–466. https://doi.org/10.1016/j.mito.2011.01.008

51. Uitterdijk A, Yetgin T, te Lintel Hekkert M, Sneep S, Krabbendam-Peters I, van Beusekom HM, Fischer TM, Cornelussen RN, Manintveld OC, Merkus D, Duncker DJ (2015) Vagal nerve stimulation started just prior to reperfusion limits infarct size and no-reflow. Basic Res Cardiol 110:508. https://doi.org/10.1007/s00395-015-0508-3

52. Wang Q, Liu GP, Xue FS, Wang SY, Cui XL, Li RP, Yang GZ, Sun C, Liao X (2015) Combined vagal stimulation and limb remote ischemic perconditioning enhances cardioprotection via an anti-inflammatory pathway. Inflammation 38:1748–1760. https://doi.org/10.1007/s10753-015-0152-y

53. Whelan RS, Kaplinskiy V, Kitsis RN (2010) Cell death in the pathogenesis of heart disease: mechanisms and significance. Annu Rev Physiol 72:19–44. https://doi.org/10.1146/annurev.physiol.010908.163111

54. Wu W, Lu Z (2011) Loss of anti-arrhythmic effect of vagal nerve stimulation on ischemia-induced ventricular tachyarrhythmia in aged rats. Tohoku J Exp Med 223:27–33. https://doi.org/10.1620/tjem.223.27

55. Xue RQ, Sun L, Yu XJ, Li DL, Zang WJ (2017) Vagal nerve stimulation improves mitochondrial dynamics via an M3 receptor/CaMKKbeta/AMPK pathway in isoproterenol-induced myocardial ischaemia. J Cell Mol Med 21:58–71. https://doi.org/10.1111/jcmm.12938

56. Yamakawa K, Rajendran PS, Takamiya T, Yagishita D, So EL, Mahajan A, Shivkumar K, Vaseghi M (2015) Vagal nerve stimulation activates vagal afferent fibers that reduce cardiac efferent parasympathetic effects. Am J Physiol Heart Circ Physiol 309:H1579–H1590. https://doi.org/10.1152/ajpheart.00558.2015

57. Yan W, Zhang H, Liu P, Wang H, Liu J, Gao C, Liu Y, Lian K, Yang L, Sun L, Guo Y, Zhang L, Dong L, Lau WB, Gao E, Gao F, Xiong L, Wang H, Qu Y, Tao L (2013) Impaired mitochondrial biogenesis due to dysfunctional adiponectin-AMPK-PGC-1alpha signaling contributing to increased vulnerability in diabetic heart. Basic Res Cardiol 108:329. https://doi.org/10.1007/s00395-013-0329-1

58. Yarana C, Sripetchwandee J, Sanit J, Chattipakorn S, Chattipakorn N (2012) Calcium-induced cardiac mitochondrial dysfunction is predominantly mediated by cyclosporine A-dependent mitochondrial permeability transition pore. Arch Med Res 43:333–338. https://doi.org/10.1016/j.arcmed.2012.06.010

59. Yellon DM, Hausenloy DJ (2007) Myocardial reperfusion injury. N Engl J Med 357:1121–1135. https://doi.org/10.1056/NEJMra071667

60. Yu L, Huang B, Po SS, Tan T, Wang M, Zhou L, Meng G, Yuan S, Zhou X, Li X, Wang Z, Wang S, Jiang H (2017) Low-level tragus stimulation for the treatment of ischemia and reperfusion injury in patients with ST-segment elevation myocardial infarction: a proof-of-concept study. JACC Cardiovasc Interv 10:1511–1520. https://doi.org/10.1016/j.jcin.2017.04.036

61. Yuan H, Silberstein SD (2016) Vagus nerve and vagus nerve stimulation, a comprehensive review: part I. Headache 56:71–78. https://doi.org/10.1111/head.12647

62. Zannad F, De Ferrari GM, Tuinenburg AE, Wright D, Brugada J, Butter C, Klein H, Stolen C, Meyer S, Stein KM, Ramuzat A, Schubert B, Daum D, Neuzil P, Botman C, Castel MA, D'Onofrio A, Solomon SD, Wold N, Ruble SB (2015) Chronic vagal stimulation for the treatment of low ejection fraction heart failure: results of the NEural Cardiac TherApy foR Heart Failure (NECTAR-HF) randomized controlled trial. Eur Heart J 36:425–433. https://doi.org/10.1093/eurheartj/ehu345

63. Zhao M, He X, Bi XY, Yu XJ, Gil Wier W, Zang WJ (2013) Vagal stimulation triggers peripheral vascular protection through the cholinergic anti-inflammatory pathway in a rat model of myocardial ischemia/reperfusion. Basic Res Cardiol 108:345. https://doi.org/10.1007/s00395-013-0345-1

64. Zhao M, Sun L, Yu XJ, Miao Y, Liu JJ, Wang H, Ren J, Zang WJ (2013) Acetylcholine mediates AMPK-dependent autophagic cytoprotection in H9c2 cells during hypoxia/reoxygenation injury. Cell Physiol Biochem 32:601–613. https://doi.org/10.1159/000354464

65. Zong H, Ren JM, Young LH, Pypaert M, Mu J, Birnbaum MJ, Shulman GI (2002) AMP kinase is required for mitochondrial biogenesis in skeletal muscle in response to chronic energy deprivation. Proc Natl Acad Sci USA 99:15983–15987. https://doi.org/10.1073/pnas.252625599

66. Zorzano A, Liesa M, Sebastian D, Segales J, Palacin M (2010) Mitochondrial fusion proteins: dual regulators of morphology and metabolism. Semin Cell Dev Biol 21:566–574. https://doi.org/10.1016/j.semcdb.2010.01.002